ACKNOWLEDGEMENTS

I would like to express my sincere gratitude to my thesis supervisor Prof. Gülay Altay, without whom this research would not have been possible. She not only provided direction and guidance through the course of this research, but she also inspired me to really learn and understand the topic of my thesis. I would also like to thank her for all of her everlasting encouragement and her continued support during this study.

I would also like to thank my academic advisory committee members, Prof. Turan Özturan and Assoc. Prof. Cavidan Yorgun for their useful suggestions and comments.

Special thanks go to my parents for their endless support and encouragement and for always believing, and helping me to believe, that I can succeed at anything. Also, I would like to thank all of the wonderful friends I have had in this university, especially to Serkan Karapınar, Mehmet Seyhan, my roommates Burcu Baykurt and Meriç Esen, who were beside me in my difficult times and made these years meaningful and enjoyable.

ABSTRACT

STEEL FRAMES UNDER FIRE

Fire resistance is the ability of a structure or a member to fulfil required functions (load-bearing capacity, and/or separating function), for a specified fire exposure and for a specified period of time. To apply fire protection to a structure, it is necessary to understand its behaviour in a real fire situation. Therefore, analytical methods are developed to predict the behaviour of fire, temperature rise in the structure and the response of the structure at elevated temperatures.

In order to analyse the steel frames under fire conditions, plastic theory has successfully adopted to the steel frames. Plastic theory can predict the collapse loads of framed structures. The fundamental theorems of plastic analyses are named as the Lower Bound Theorem, Upper Bound Theorem and Uniqueness Theorem. These three theorems are also used successfully under fire conditions. As these theorems are used for the calculation of the critical temperatures and their possible distribution at collapse under fire conditions, also the Rankine Approach can be used for the same purpose as well. Second order analyse which is another method to find the critical temperature considering the axial load effects, has to be taken into account during the analyses, too.

The aim of this study is to give information about the overall process of designing structures for fire exposure. It also provides the information needed for calculating the performance of steel buildings exposed to fires. Simple methods are described for determining the critical temperatures for individual steel members to resist fire exposure, including calculations of elevated temperatures and information on the thermal and mechanical properties of steel at elevated temperatures. Fire behaviour of steel structures is also discussed.

ÖZET

ÇELİK ÇERÇEVELERİN YANGIN ETKİSİ ALTINDA ANALİZİ

Yangına dayanıklılık bir yapının veya elemanının istenilen görevleri (taşıma kapasitesi ve/veya diğer görevler) belirli bir yangın anında ve belirli bir zaman aralığında yerine getirebilme yeteneğidir. Bir yapıya yangına karşı koruma yöntemleri uygulamak için, o yapının gerçek bir yangın anındaki davranışını anlamak gereklidir. Bu yüzden, günümüzde yangının davranışını, yapıdaki sıcaklık artışını ve yapının yüksek sıcaklıklara karşı tepkisini önceden anlamak için birçok analitik metotlar geliştirilmiştir.

Yangın etkisi altındaki çelik çerçevelerin analizi için plastic teori çelik çerçevelere başarıyla uygulanmaktadır. Plastik teori yardımıyla çerçeveli yapıların çökme yükü önceden belirlenebilmektedir. Yangın etkisi altındaki plastik analizlerin temel teoremleri; Alt Sınır Teoremi, Üst Sınır Teoremi ve Eşdeğer Teorem olarak adlandırılmıştır. Bu teoremler kritik sıcaklıkları ve yangın durumunda sıcaklığın çökme anındaki muhtemel dağılımının hesaplamalarında kullanıldığı gibi, ayrıca bir başka yöntem olan Rankine yaklaşımı da aynı amaç için kullanılabilmektedir. Yanal yük etkileri gözönüne alınarak kritik sıcaklık bulmak için kullanılan bir diğer yöntem ise 2. Mertebe Analizidir. Bütün bu analizler yapılırken, 2. Mertebe Analizinin de hesaba katılması gerekmektedir.

Bu tezin amacı; yangına maruz kalmış yapıların dizayn metotlarının ayrıntılı olarak incelenmesidir. Ayrıca bu çalışma yangına maruz kalmış çelik yapıların dayanımının hesaplanması için gereken bilgiyi de sağlamaktadır. Çelik elemanların yangına karşı dayanımını sağlamak için, bu elemanların kritik sıcaklıklarının belirlenmesinde kullanılabilecek basit yöntemler açıklanmıştır. Ayrıca yüksek çökme sıcaklıklarının hesabı, çeliğin yüksek sıcaklıklardaki termal ve mekanik özellikleriyle ilgili bilgiler de verilmiştir. Çelik yapıların yangın karşısındaki davranışı da ayrıca açıklanmıştır.

TABLE OF CONTENTS

LIST OF FIGURES

LIST OF TABLES

LIST OF SYMBOLS/ABBREVIATIONS

A	Cross sectional area
A_0	Ground acceleration coefficient
$A(T)$	Spectral acceleration coefficient
A_b	Area of the beam section
A_c	Area of the column section
A_v	Shear area
c_c	Specific heat of concrete
c_p	Specific heat
c_s	Specific heat of steel
C_t	Building period of coefficient
D	Depth of the section
$\{D\}$	System deformation matrix
E	Elasticity of modulus
E_x	Earthquake load acting in x direction
e_i, e_j, e_{ij}	Stability function coefficient
f_y	Yield strength at 20°C
$f_{y,T}$	Yield stress at elevated temperature
Σf	Total fixed end reaction vector
G	Dead load
G	Unit weight of section
H_n	Total height of the building
h	Column height
I	Moment of inertia
I	Occupancy importance factor
$[K]$	System stiffness matrix
k	Stability function in the x-y plane
$k_{E,T}$	Reduction factor of modulus of elasticity due to temperature
$k_{y,T}$	Reduction factor of yield strength due to temperature
L	Length of structural member
$\Delta L/l$	Thermal elongation

m	Equivalent uniform moment factor
M	Equivalent uniform moment
M_b	Buckling resistance moment
M_c	Moment capacity
M_p	Plastic moment capacity
$M_{p,T}$	Plastic moment capacity at elevated temperature
n	Curve fitting coefficient
n	Slenderness correction factor
P	Axial force causing instability
p_b	Bending strength
P_c	Compressive resistance
p_c	Compressive strength
p_y	Design strength
Q	Live load
q	Wind pressure
R	Response modification factor
R	Load ratio
r_x, r_y	Radius of gyration for x-x and y-y axis
$S(T)$	Spectrum coefficient
S	Plastic modulus of section
T	Temperature
T_A	Spectrum characteristic period
T_B	Spectrum characteristic period
T_c	Critical temperature of collapse
T_1	Natural period of vibration
t	Total web thickness
ΔT	Temperature change
u	Buckling parameter of the section
V_t	Equivalent earthquake force
v	Slenderness factor
W	Total mass of the structure
W	Wind load
Z4	Site class

α	Curve fitting coefficient
α	Temperature factor
α_t	Expansion coefficient
Δ	Deflection
δ	Horizontal deflection
ε	Strain
ε_{cr}	Creep strain
ε_{th}	Thermal strain
ε_{tth}	Transient thermal strain
θ_a	Material temperature
λ	Slenderness factor
λ	Thermal conductivity
λ_c	Thermal conductivity of concrete
λ_c	Critical load factor
λ_e	Elastic buckling load factor
λ_p	Plastic collapse load factor
σ	Stress
ϕ_c	Stability function under compression
Ω_0	System over strength factor

BSI	British Standard Institute
EC2	Eurocode 2
EC3	Eurocode 3
EC4	Eurocode 4
TS	Turkish Standards Institute
UB	Universal beams
UC	Universal columns

1. INTRODUCTION

1.1. Introduction

Fires in buildings have always been a threat to human safety. The threat increases as larger numbers of people live and work in larger buildings throughout the world. Unwanted fire is a destructive force that causes many thousands of deaths and billions of dollars of property loss each year. People around the world expect that their homes and workplaces will be safe from the ravages of an unwanted fire. Unfortunately, fires can occur in almost any kind of building, often when least expected. The safety of the occupants depends on many factors in the design and construction of the buildings, including the expectation that certain buildings and parts of buildings will not collapse in a fire or allow the fire to spread.

After the horrific September 11^{th} terrorist attack on the World Trade Center which caused the collapse of the building and the deaths of thousands of people, it is estimated that there is an increase in the need of a rational, easy, performance-based approach to the problem of resistance and stability of steel frames under fire conditions.

The analysis of steel frames under fire conditions has been a question to scholars and researchers since the demand for a rational performance-based approach of structures under elevated temperatures has increased. To apply fire protection to a structure, it is necessary to understand its behaviour in a real fire situation. Therefore, it is important to develop a package of analytical methods to predict the behaviour of fire, temperature rise in the structure and the response of the structure at elevated temperature.

Design to provide fire safety is based on scenario analysis. For any scenario it is possible to calculate some responses, but the level of accuracy can only be as good as the design assumptions, the input data and the analytical methods available.

In recent years, many design codes have progressively abondened the conservative and prescriptive approaches for fire design of structures. Several codes of practice have

also permitted the use of plastic theory which is one of the important methods in fire analysis as well. Plastic theory has since been successfully applied to the designs of flexural members and framed structures at ambient temperature. This theory is also used for the structures which are at elevated temperature as well.

Full-scale fire tests on structures are now possible with realistic loading and environmental conditions to assess the actual behaviour of frames and their components. Sophisticated mathematical modelling and simulation of the structural and thermal interactions in the structures contribute to these tests as the high cost of testing is taken into account. In contrast, simplified procedures and methods for analysis of steel frames under fire conditions have been widely adopted in many design codes. These simplified procedures, methods and empirical formulas usually make convenient assumptions and give close results.

1.2. Literature Review

Wang *et al.* (1995) developed a finite element computer program which is studying the structural behaviour of steel frames at elevated temperatures. The program permits the calculation of the load-deflection response of steel frames at cold condition and their behaviour at elevated temperatures under constant loading. The effects of nonlinear material properties, second order effects of large deflections and the behaviour of flexible beam-column connections are included. Both uniform and non-uniform temperature distributions are applied in the analyses. A novel feature of the analyses is the inclusion of the behaviour of semi-rigid, beam-column connections. Both 2D and 3D frames can be analysed with the help of this program, although only 2D frames have been validated. Additionally, using this program, a number of tests performed on various types of construction at ambient temperature or elevated temperature were studied. Apart from demonstrating the accuracy and capacity of the computer program, these studies show that the behaviour of an individual member in fire is different from that of the same member active as part of a frame. The predictions using the computer program and the test results of frames in fires are also compared. It is believed that when this program is used in conjuction with other analytical methods to predict the behaviour of real fires and

temperature rises in structures, the behaviour of steel frames in real fires can be correctly predicted.

Toh *et al.* (2001) presented a second order elastic plastic hinge method and a finite element model for the analysis of plane frames in fire. They give the extension of the three classical plastic theorems, viz, the Lower Bound Theorem, Upper Bound Theorem and Uniqueness Theorem, to structural analysis incorporating thermal effects. The three plastic theorems are given in new definitions, followed by original mathematical proofs. The proposed finite-element model has been validated against a series of published test and analytical results on different structure types. For comparison purposes, numerical examples are presented to examine the relative performance of the three methods investigated in the study as well.

While presenting the numerical examples to investigate the performance of the various methods proposed, it is examined on the frames whether the methods can deal with thermal strains and geometric nonlinearity. Also, the steel stress-strain relationships at elevated temperature in the finite element model is used for the material models.

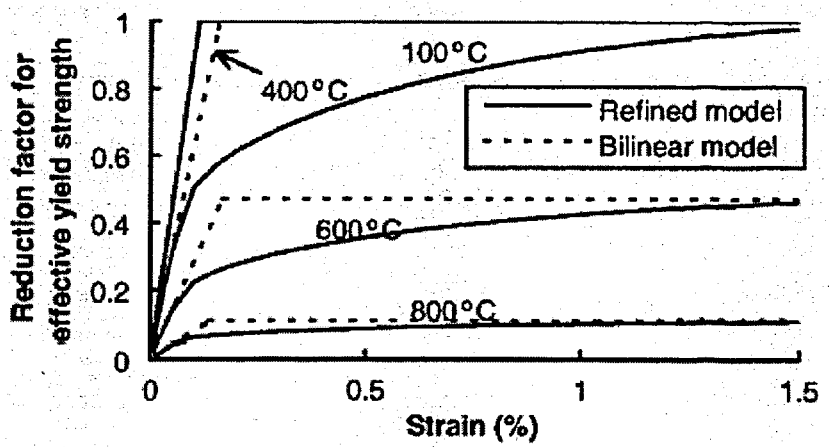

Figure 1.1. Steel material model at elevated temperatures (Toh *et al.*, 2001)

The steel stress-strain relationships at elevated temperatures in the finite element members are adopted from Eurocode 3 (EC3-1.2), as represented by the solid curves in Figure 1.1. In the plastic hinge analysis, the steel stress-strain relationships in the code are simplified to be bilinear shapes, represented by the dotted lines in Figure 1.1. The code

reduction factors for the slope of the linear elastic range and the effective yield strength are applied to elastic modulus and yield strength, respectively.

Franssen *et al.* (1994) and Sullivan *et al.* (1994) provide extensive reviews and comparisons of many of the existing finite-element models for structural fire protection applications. According to Sullivan *et al.* (1994), all of the models include the following assumptions:

- The Navier-Bernoulli hypothesis: plane sections remain plane
- Slippage between the steel and the concrete is neglected
- Torsion is neglected

Sullivan *et al.* (1994) review the following eight finite-element models:

- FASBUS-II (Jeanes 1982)
- FIRES-RCII (Iding et al. 1977)
- CONFIRE (Forsen 1982)
- STEELFIRE (Forsen 1983)
- CEFICOSS (Franssen 1987)
- LUSAS (*LUSAS* 1988)
- Sheffield/Nethercot (Nethercot, personal communication to Sullivan *et al.*, 1988)
- BRE (Yong, personal communication to Sullivan *et al.*, 1990)

The review of the models is conducted by reviewing the documentation for the models, concentrating on their formulation and basis. As a result of the review, Sullivan *et al.* (1994), provide the following comments:

- The predictive capability of the structural models is less than that for the thermal finite-element models due to inadequate material models, uncertain material property values and sensitivity of the structural response to elevated temperatures.
- The stress history of an assembly is ignored.
- Transient thermal creep in concrete is ignored, having its greatest impact on concrete columns.

- Creep is compensated for by defining other mechanical properties as "effective" properties.
- Because the models are based on the Navier-Bernoulli assumption of small displacements, large displacements are not accurately modeled.

Toh *et al.* (2001) proposed a simple analytical approach based on the Rankine principle which has been developed to determine the ultimate resistance of steel frames in fire. The proposed Rankine approach gives an approximation of the frames' fire resistance through a simple interaction between two idealized structural behaviours; strength and stability. In the proposed approach, the strength and stability of the structures are evaluated using the rigid-plastic and the elastic buckling analyses, both incorporating the thermal effects. The proposed approach is first verified using a finite-element model. The verification studies include the effects of column and frame slenderness ratios, beam-column stiffness ratio, steel grades, initial sway imperfections, and initial residual stresses. These studies indicate that frame slenderness ratio is an important parameter governing the behavior of simple frames in fire and the performance of the proposed approach is related to it.

At each particular temperature T, the proposed Rankine approach allows the strength and the stability aspects of a steel frame to be separately determined. The rigid-plastic collapse load factor λ_p is used to define the frame strength, while the elastic buckling load factor λ_e governs the frame stability. For a frame subjected to proportional loading, the interaction of these two idealized load factors gives rise to the critical load factor λ_c at temperature T, as follows in the Equation 1.1:

$$1/\lambda_c(T) = 1/\lambda_p(T) + 1/\lambda_e(T) \qquad (1.1)$$

Alternatively, if the critical temperature T_c is of interest while the applied working loads remain constant ($\lambda_c(T_c) = 1.0$), a trial-and-error procedure is necessary to determine T_c such that the sum of $1/\lambda_P(T_c)$ and $1/\lambda_e(T_c)$ is equal to unity. Figure 1.2 illustrates the variation of λ_c versus T for a frame at elevated temperatures.

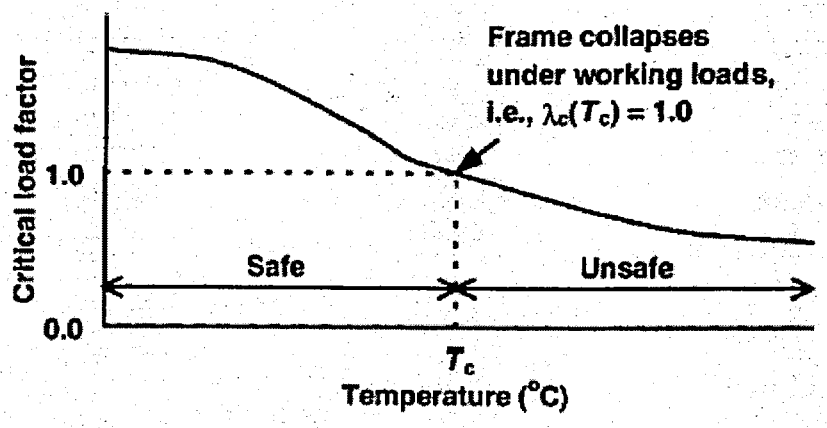

Figure 1.2. Variation of critical load factor with respect to temperature (Toh *et al.*, 2001)

So, a preliminary study of the effects of various parameters on the accuracy of the Rankine approach is presented in this study. The proposed Rankine approach results and the test results showed the accuracy when the comparison was made. Also, it is seen that a consistently good agreement with both numerical and test results shows that the proposed Rankine approach can be utilized as a quick tool to assess the fire resistance of steel frames fully exposed to fire above 400°C.

2. MATERIAL PROPERTIES AT ELEVATED TEMPERATURE

The mechanical properties of steel and concrete at elevated temperatures are different from their properties at room temperature due to the temperature dependent stress-strain relationships and temperature induced strains. To accurately, predict the response of structures under fire conditions, correct models of stress-strain-temperature relationships and temperature induced strains should be used. The various high temperature material properties for steel and concrete adopted in the present analysis will be briefly described below.

2.1. Material Properties of Steel

2.1.1. Stress-Strain-Temperature Relationship

Three models are used to represent the stress-strain relationship at elevated temperature for steel. They are the tabulated British Steel test results, the Ramberg-Osgood Curve-fitting equations to the British Steel test results and the mathematical model proposed in European Steel Structure Design Code (Eurocode) for fire resistance.

In the British Steel tabulated test results stress-strain data are provided for Grade 43A and 50B steels with yield stresses at room temperature being 275 N/mm^2 and 355 N/mm^2 for temperatures up to 800°C and strains up to 2%. In the present analysis, it is assumed that steel melts at 1300°C thus, possessing no strength. Stress-strain relationships for steels of different room temperature yield stresses and temperature values between 800°C and 1300°C are obtained by interpolation.

Using the Ramberg-Osgood formulae, strains may be expressed as a function of stresses as follows;

$$\varepsilon=\sigma/E+\alpha\,(\sigma/E)^{n} \qquad (2.1)$$

where, E is the initial tangent of the stress-strain curve at elevated temperature and α, n are the curve fitting coefficients.

In the European steel structure design code for fire resistance, the stress-strain curves at elevated temperatures are described by a linear-elliptic-linear equation which assumes that stress increases linearly up to the limit of proportionality and then the curve follows an elipse until a maximum stress corresponding to a strain of 2%. Afterwards, plastic flow forms until the strain reaches 20%. This stress-strain relationship is illustrated in the Figure 2.1 below. Values of stress at the limit of proportionality and the maximum stress in terms of the steel yield stress at room temperature together with the reduction of Young's Modulus at elevated temperature are given in Eurocode 3.

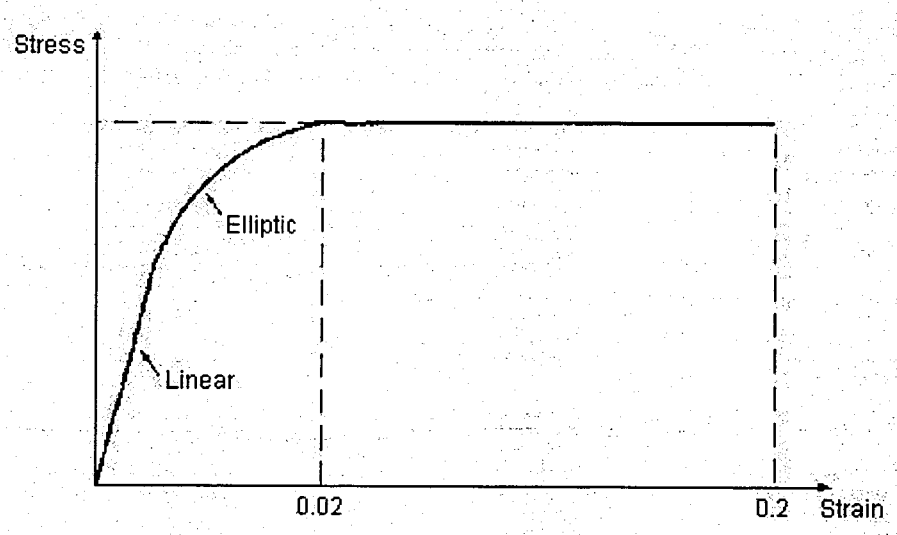

Figure 2.2. Stress-strain relationship for steel at elevated temperature (Wang *et al.*, 1995)

It is assumed that steel has identical material properties in both tension and compression. Unloading is assumed to follow the initial slope of the stress-strain curve at elevated temperature with a permanent plastic strain.

2.1.2. Temperature Induced Strains

For steel, the thermal strains include thermal expansion (ε_{th}) and creep strain (ε_{cr}). Thermal expansion depends on the temperature increase only. The increase in thermal expansion maybe assumed to be linear with temperature increase. The coefficient of

thermal expansion varies from 12x10E-6 at room temperature to 15x10E-6 at about 800°C. Creep strain is a function of temerature, stress level and time.

2.2. Material Behaviour of Steel in Fire

When a steel structure is exposed to a fire, the steel temperatures increase and the strength and the stiffness of the steel are reduced, leading to possible deformation and failure, depending on the applied louads and the support conditions. The increase in steel temperatures depends on the severity of the fire, the area of steel exposed to the fire and the amount of applied fire protection. There are many methods of protecting steel members from the effects of fire, so that the structural steel buildings with applied fire protection can be designed to have excellent fire resistance.

Unprotected steel structures tend to perform poorly in fires compared with reinforced concrete or heavy timber structures, because the steel members are usually much thinner. Steel also has a higher thermal conductivity than most other materials. Unprotected steel structures can survive some fires if the severity is low and the steel does not get too hot. Full-scale tests and some real fires in large steel buildings have shown that well-designed strctures can resist severe fies without collapse, even if some of the main load-bearing members are unprotected. Thermal expansion of steel members can cause damage elsewhere in the building.

The main factors affecting the behaviour of steel structures in fire are as follows;

- The elevated temperatures in the steel members
- The applied loads on the structure
- The mechanical properties of the steel and
- The geometry and the design of the structure

When subject to fire, an unprotected steel structure will loose its stiffness and strength as a result of deterioration in its material properties. The traditinal approach to this problem is to design the structure for ambient temperature and apply various insulation

techniques to its load-bearing members to meet the recommendaions for fire resistance. The fire resistance of a load-bearing member is based on the results of standard fire tests.

In these tests, a simply supported load-bearing member under its maximum design stress is heated in a Standard fire test furnace according to a standard fire exposure. The time taken for the member to reach a prescribed failure criterion is the fire reistance of the member. It is generally believed that such a design method has the following deficiencies;

- Only test specimens which represent small to medium size construction can be tested.
- Different characteristics of various furnaces hinder the international exchange of standard fire resistance test results.
- The standard fire exposure curve does not represent the characteristics of real fires.
- The behaviour of an isolated member subject to idealized loading and boundary conditions differs significantly from that of a member within a complex, highly redundant structure.

Therefore, the fire resistance of a load-bearing member (the ability to maintain loadbearing capacity in fire) obtained from a Standard fire test can be significantly different from the fire resistance of the same member within a complete structure in a real fire. It follows that the fire resistance of the member should be assessed from real fire tests on full scale structures. However, the costs of such tests are prohibitive. Alternatively, the fire resistance of structural members may be obtained using analytical approaches. For such an analysis to be performed requires an understanding of the growth of a real fire, the temperature attained in the structure and the behaviour of the structure under fire condition.

2.3. Material Properties of Concrete

2.3.1. Stress-Strain-Temperature Relationship

The stress-strain behaviour of concrete in compression is assumed to follow a parabola until maximum compressive strength, followed by a plateau at this maximum compressive stress until crushing occurs. Concrete behaviour in tension is linear until its

maximum tensile strength is reached, followed by a gradual decrease in tensile stress with increasing tensile strain until cracking. Figure 2.2 shows this relationship. This behaviour of concrete is followed at both room and elevated temperatures. However, the compressive strength, tensile strength and Young's modulus of the concrete are reduced at elevated temperatures.

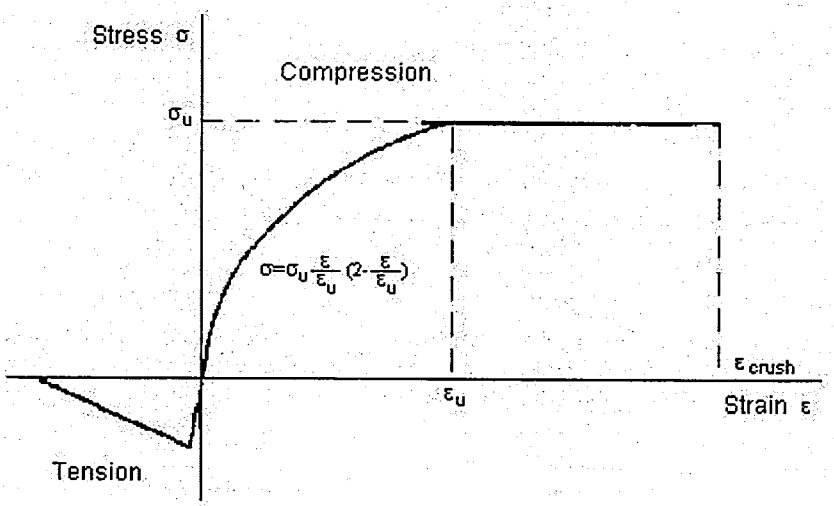

Figure 2.1. Stress-strain relationship for concrete at elevated temperature (Wang *et al.*, 1995)

2.3.2. Temperature Induced Strains

Thermal strains of concrete include thermal expansion (ε_{th}), creep strain (ε_{cr}) and transient thermal strain (ε_{tth}).

3. THERMAL PROPERTIES OF MATERIALS

The prediction of temperature distribution of the fire, exposed structural member is one important step in the design process. The reliability of computed temperature is dependent on accurate and sufficient knowledge about the thermal properties of building materials used. Properties normally used in computer programs are thermal conductivity and volumetric specific heat (c_p, ρ). These properties are relatively easy to determine for steel but for concrete it is far more difficult especially as concerns the thermal conductivity.

3.1. Thermal Properties of Steel

3.1.1. Thermal Conductivity

The thermal conductivity is dependent on steel composition as well as the steel temperature. The thermal conductivity of reinforcing steel has a very high value 54 W/mK at room temperature and is then decreasing to 27.3 W/mK at 800°C. The thermal conductivity of stainless steel is very different and has a low value 14.6 W/Mk at room temperature and increases nearly to 30 W/Mk at 1200°C in accordance with Eurocode 3. The thermal conductivity of stainless steel is very different from reinforcing and prestressing steel. The thermal conductivity for stainless steel is much lower than reinforcing steel and is constantly increasing by temperature when reinforcing steel is decreasing from a value more than three times higher. This means that below 950°C stainless steel is conducting heat slower than reinforcing steel. The equations for thermal conductivity from Eurocode (EC3:1995) are shown below. Also the thermal conductivity of steel as a function of temperature is given in Figure 3.1.

$$\lambda = 54 - 3.33E\text{-}2 * \theta_a \quad \text{(W/Mk)} \qquad \text{For } 20°C \leq \theta_a < 800°C \tag{3.1}$$

$$\lambda = 27.3 \quad \text{(W/Mk)} \qquad \text{For } 800°C \leq \theta_a < 1200°C \tag{3.2}$$

where, θ_a is the material temperature.

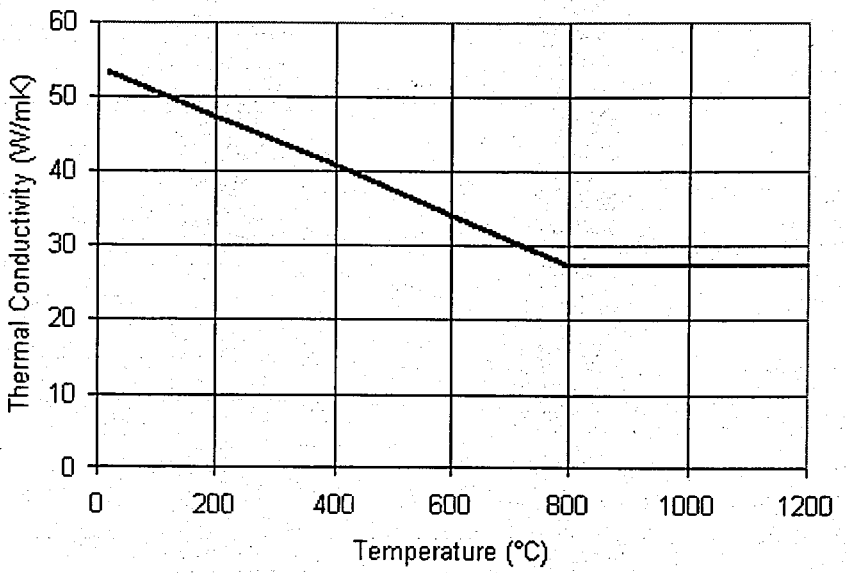

Figure 3.1. Thermal conductivity of steel as a function of temperature

3.1.2. Specific Heat and Density

The figure shows that the specific heat of steel varies with temperature. The specific heat of steel is independent of steel composition. Specific heat is the ability of the steel to absorb heat.The specific heat of reinforcing steel c_s is increasing from about 425 J/kgK at room temperature up to 600 J/kgK at 1200°C but it has a peak at 735°C which ends at 5000 J/kgK. The specific heat of stainless steel as presented in Eurocode 3 is somewhat lower than for reinforcing and prestressing steel and the peak at 735°C for normal steel does not exist for stainless steel. This means that stainless steel per weight needs somewhat less energy to be heated up than normal steel.The equations from the Eurocode (EC3:1995) for the specific relationships are shown below. Specific heat of steel as a function of temperature is given in Figure 3.2 as well.

For $20°C \leq \theta_a < 600°C$ J/kgK;

$$c_s = 425 + 7.73E\text{-}1 * \theta_a - 1.69E\text{-}3 * \theta_a * 2 + 2.22E\text{-}6 * \theta_a * 3 \quad (3.3)$$

For $600°C \leq \theta_a < 735°C$ J/kgK;

$$c_s = 666 + 13002/(738 - \theta_a) \quad (3.4)$$

For $735°C \leq \theta_a < 900°C$ J/kgK;

$$c_s = 545 + 17820/(\theta_a - 731) \quad (3.5)$$

For $900°C < \theta_a$ J/kgK;

$$c_s = 650 \quad (3.6)$$

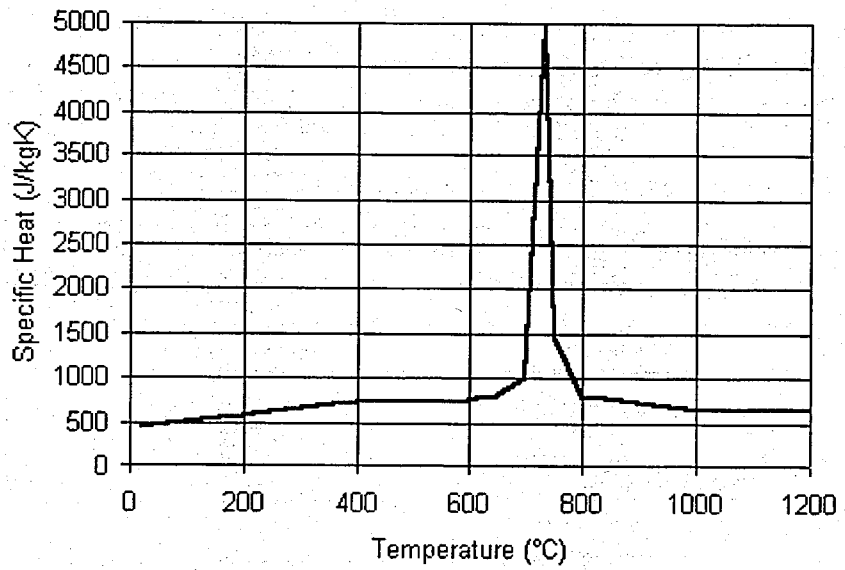

Figure 3.2. Specific heat of steel as a function of temperature

3.1.3. Thermal Elongation ΔL/ l

The thermal elongation of steel ΔL/l is determined from the following equations from the Eurocode (EC3:1995). The discontinuity in the thermal elongation is due to a phase transformation that occurs in the steel in the temperature range between 750°C and 860°C as shown in Figure 3.3 below.

$$\Delta L/l = 1.2E\text{-}5*\theta_a + 0.4E\text{-}8*\theta_a^2 - 2.416E\text{-}4 \quad \text{For } 20°C \leq \theta_a < 750°C \quad (3.7)$$

$$\Delta L/l = 1.1E\text{-}2 \quad \text{For } 750°C \leq \theta_a < 860°C \quad (3.8)$$

$$\Delta L/l = 2E\text{-}5*\theta_a - 6.2E\text{-}3 \quad \text{For } 860°C \leq \theta_a < 1200°C \quad (3.9)$$

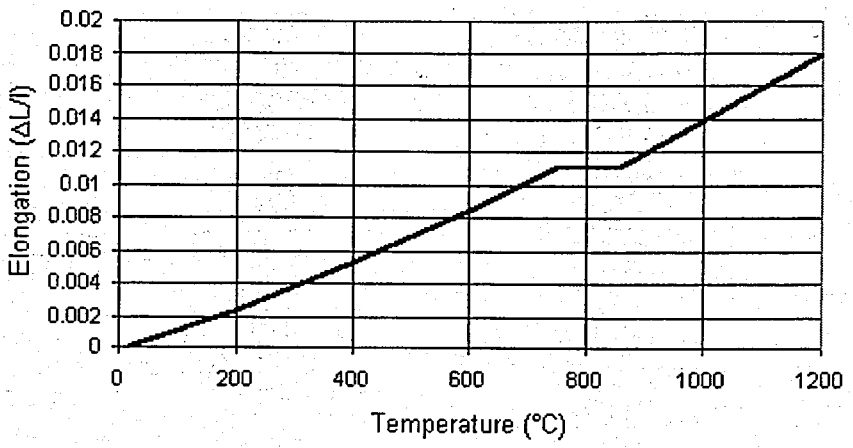

Figure 3.3. Thermal elongation of steel as a function of temperature

3.2. Thermal Properties of Concrete

3.2.1. Thermal Conductivity

Thermal conductivity as function of high temperature is very difficult to measure due to the influence of many parameters as moisture content and its continous movement, the type and amount of aggregate etc. Furthermore measurement methods and devices are not sufficiently accurate to be fully trusted. Steady state tests are normally applied neglecting the dynamic temperature and moisture condition, which consequently create a measuring problem. Unfortunately in most countries testing standards do not exist.

Due to the uncertanity to measure thermal conductivity, the only way to judge about the correctness is to simulate fire tests and compare measured temperature values all over the cross-section with computed values based on measured thermal conductivity and by a fixed volumetric specific heat curve.

The composition of concrete and the types of aggregate used have an influence on thermal conductivity. The curve presented below is valid for siliceous concrete and is on the safe side when used for calcareous concrete. The conductivity curve is valid for the first heating and cooling down the value attained at maximum temperature remain during cooling.

In Eurocode 2 (2002) and Eurocode 4 (2003) a compramise has been made so that the thermal conductivity can be chosen between an upper and a lower limit as shown in Figure 3.4. This is of course an undesirable solution when concrete must have the same properties in reinforced concrete as in composite concrete-steel structures.

The upper limit of thermal conductivity λ_c of normal weight concrete may be determined from:

For $20°C \leq \theta_a \leq 1200$;

$$\lambda_c = 2 - 0{,}2451*(\theta_a/100) + 0{,}0107*(\theta_a/100)^2 \quad W/mK \tag{3.10}$$

The lower limit of thermal conductivity λ_c of normal weight concrete may be determined from:

For $20°C \leq \theta_a \leq 1200$;

$$\lambda_c = 1{,}36 - 0{,}136*(\theta_a/100) + 0{,}0057*(\theta_a/100)^2 \quad W/mK \tag{3.11}$$

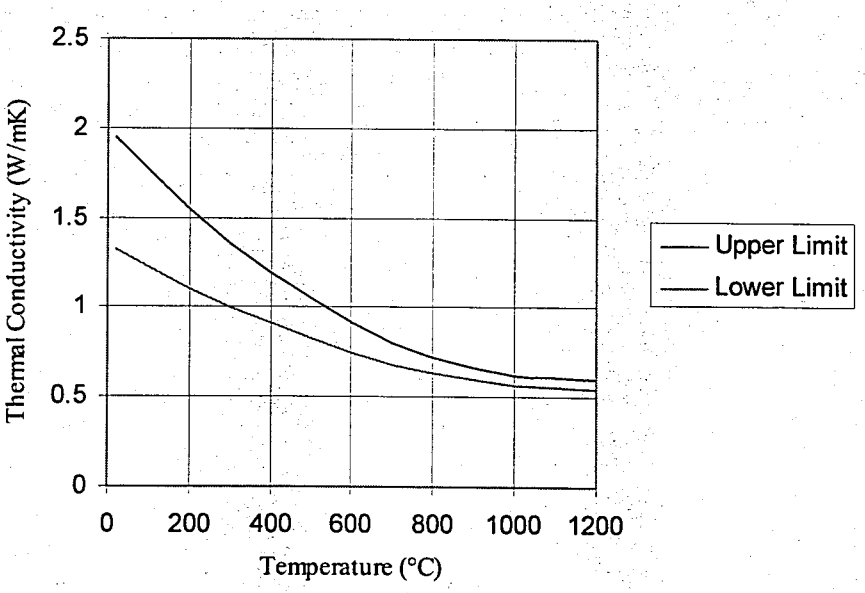

Figure 3.4. EC2 Thermal conductivity of siliceous aggregate concrete as a function of temperature

3.2.2. Specific Heat

The specific heat of concrete (c_c) varies over a broad range depending on the moisture content which for EC2 concrete is a maximum of 2%. The following relationships show the EC2 concrete specific heat. Between 100°C and 200°C there is a peak in specific heat due to water being driven off as shown in Figure 3.5.

For $20°C < \theta_a \leq 1200$;

$$c_c = 900 + 80\theta_a/120 - 4*(\theta_a/120)^2 \quad J/kgK \tag{3.12}$$

Between 100°C and 200°C there is a peak in specific heat due to water being driven off;

$c_{c,peak}$ = 1875 J/kgK for a humidity of 2% of concrete weight

$c_{c,peak}$ = 2750 J/kgK for a humidity of 4% of concrete weight

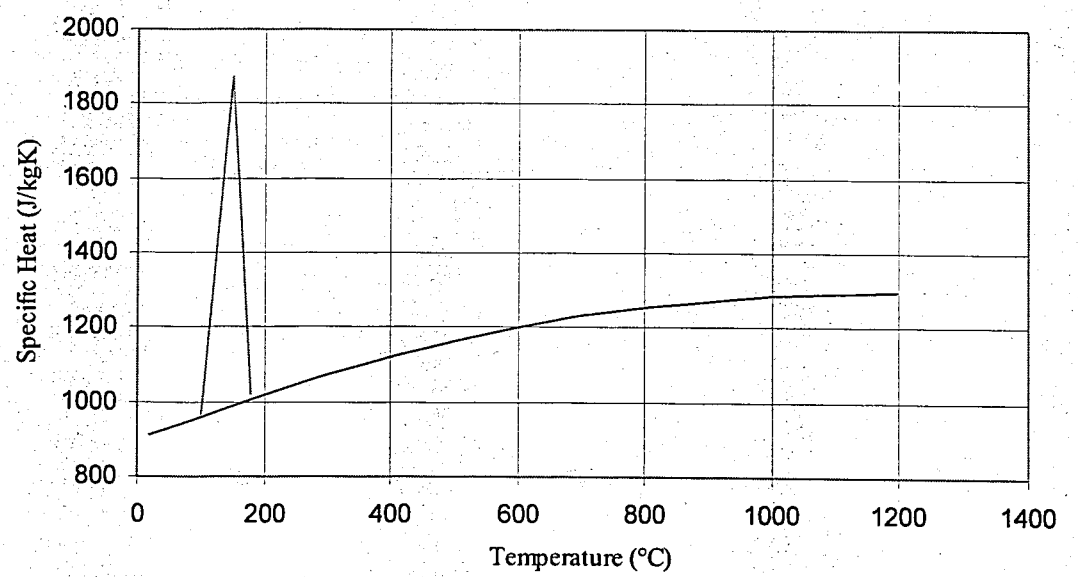

Figure 3.5. EC2 Specific heat of concrete as a function of temperature

3.2.3. Thermal Elongation ΔL/ l

The relationship below and Figure 3.6 show the thermal elongation of siliceous concrete as a function of temperature as propesed by the Eurocode (EC2:1993). This model is nonlinear up to 700°C where it becomes constant.

For $20°C < \theta_a \leq 700$;

$$(\Delta L/ l)_c = (-1{,}8E\text{-}4) + (9E\text{-}6 * \theta_a) + (2{,}3E\text{-}11\ \theta_a^3) \quad (3.13)$$

For $700°C < \theta_a \leq 1200$;

$$(\Delta L/ l)_c = 14E\text{-}3 \quad (3.14)$$

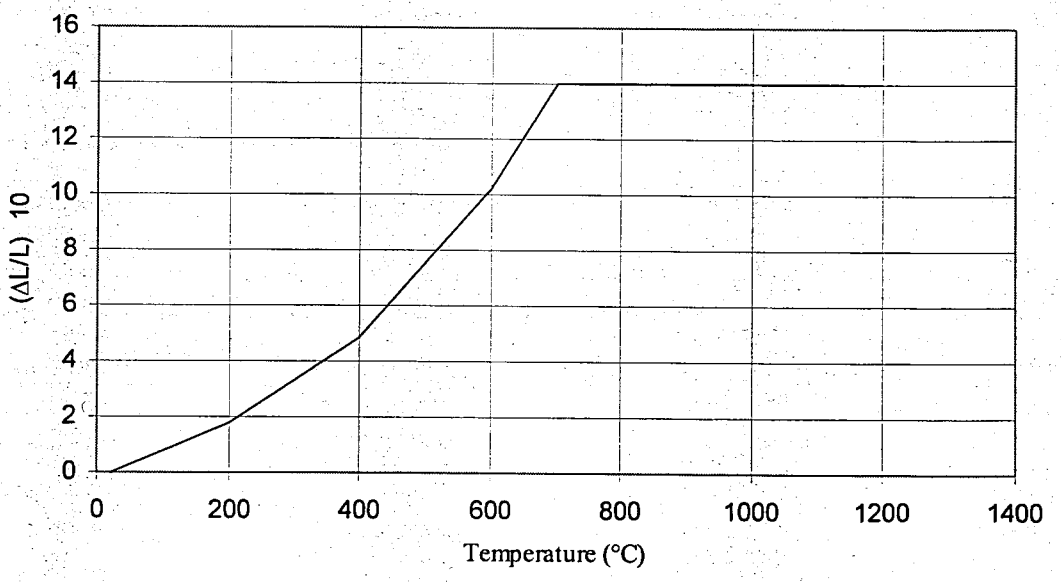

Figure 3.6. Thermal elongation of concrete as a function of temperature

4. METHODS USED FOR FIRE RESISTANCE OF STEEL FRAMES

4.1. Theorems of Plastic Collapse

The plastic theory can predict the collapse loads of framed structures by tracing the development of plastic hinges until a mechanism is formed. They are concerned with strength only and do not assess other criteria such as deflection or stability.

Under increasing temperature, all building materials are susceptible to progressive deterioration. Consider the behaviour of a steel frame subjected to fire; the steel material properties such as yield strength and elastic modulus deteriorate quickly. As a result, the plastic moment of resistance M_p also reduces. Plastic hinges will form when the M_p of the structural members deteriorates to the value of the bending moment across the section. Redistribution of stresses commences as M_p further reduces. Eventually, when sufficient plastic hinges are formed, the frame collapses as it turns into a mechanism. It should be recognized that the plastic analysis of a frame in fire is different from that under normal conditions. Instead of determining the collapse load factor λ_p subjected to incremental working loads at ambient temperature, the collapse (or survival) temperature T_c (or time) is of interest while the applied working loads remain constant. This means that, at T_c, the collapse load factor attains unity ($\lambda_p(T_c)=1.0$).

Figure 4.1 illustrates the variation of λ_p with respect to T of a structure at elevated temperatures. At any $T< T_c$, the structure remains safe under its working loads as it has not attained the collapse load yet. When T rises to T_c, the structure turns into a collapse mechanism and partial or overall collapse may occur. At any $T> T_c$, the structure is unsafe as the full plastic moment capacity has deteriorated so much that even the working loads can not be sustained.

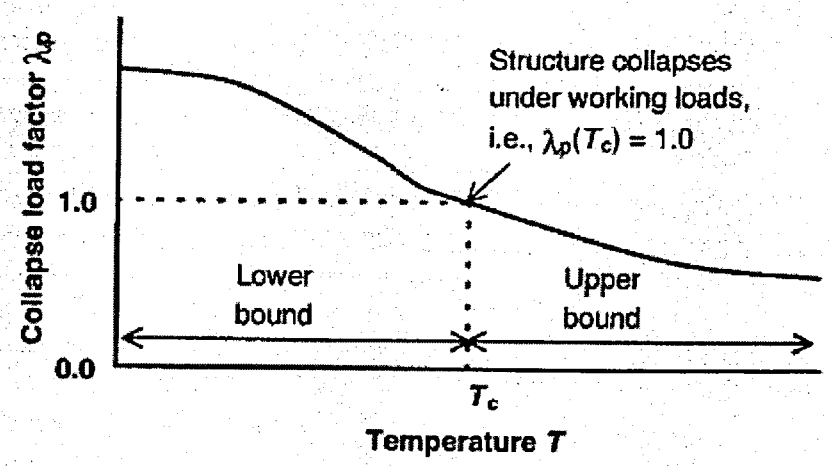

Figure 4.1. Variation of critical load factor with respect to temperature

To apply the methods of plastic analysis under thermal effects, several important assumptions underlying the plastic theorems are as follows:

- The temperature increases monotonically with time.
- The structure is made of ductile materials capable of achieving full plastic moment of resistance and stress redistribution.
- The structural behaviour is idealized to be rigid perfectly plastic; mechanism deformations are assumed to be infinitesimal so that they have no effect on the equations of equilibrium at any temperature.
- The structure only fails by mechanisms, and the plastic moment of resistance is the only governing strength criterion. Other, phenomena, such as instability are not considered.
- The structure is subjected to constant working loads.
- Temperature distribution is uniform within the heated structural members.

4.1.1. Lower-Bound Theorem

If at any temperature T, it is possible to find a bending moment distribution in equilibrium with the applied working loads and everywhere satisfying the yield condition, then the temperature T is either equal to or smaller than the actual collapse temperature T_c. $T \leq T_c$

Hence, any temperature T so found is a lower bound on the collapse temperature T_c. In other words, T_c is the maximum possible temperature such that it is still possible to find a bending moment distribution satisfying both the equilibrium and the yield conditions. Therefore, the collapse temperature of a structure can not be decreased by increasing the strength of any part of the structure.

4.1.2. Upper-Bound Theorem

If any assumed mechanism, the external work done by the working loads is equal to the internal work at the plastic hinges, then the temperature T corresponding to the formation of the particular plastic moments is either equal to or greater than the actual collapse temperature T_c. $T \geq T_c$

Hence, any temperature T so found is an upper bound on the collapse temperature T_c. In other words, T_c is the minimum possible temperature at which a mechanism exists with equal internal or external work done. As the plastic moment of resistance decreases monotonically with increasing the temperature, it can be concluded that $T \geq T_c$. The collapse temperature of a structure can not be increased by decreasing the strength of any part of the structure.

4.1.3. Uniqueness Theorem

If the plastic moment capacity decreases monotonically as temperature increases $\partial M_p(T)/\partial T<0$, and at any temperature T, a bending moment distribution can be found that satisfies the three conditions of equilibrium, yield and mechanism, then the temperature T is the actual collapse temperature T_c. $T= T_c$

In short, the uniqueness theorem simply states that the collapse temperature determined from the three conditions of equilibrium, yield and mechanism is unique. Also, it is seen that the initial stresses have no effect on the collapse temperature. So, the collapse temperature is independent of initial stresses.

4.2. Rankine Approach

The Merchant-Rankine approach is one of the most famous approaches for frames at ambient temperatures. Based on the emprical formula originally proposed by Rankine in 1866 for perfectly straight columns, Merchant (1954) developed a more generalized formula to determine the failure load factor of rigid-jointed frames subject to proportional loading at ambient temperature. Later, Horne (1960, 1963) further investigated the fundamental principals and applications of Rankine approach.

Rankine approach can be extended to frames subjected to thermal effects. The extended approach allows the interaction between the two idealized load factors for rigid-plastic λ_p and the elastic analysis λ_e, to determine an approximation to the actual critical load factor λ_c. Basically, the thermal effects leading to the deterioration of material properties and additional axial compressive stresses in the system are the main concern.

At each particular temperature T, the proposed Rankine approach allows the strength and the stability aspects of a steel frame to be seperately determined. The rigid plastic collapse load factor λ_p is used to define the frame strength, while the elastic buckling load factor λ_e governs the frame stability. For a frame subjected to proportional loading, the interaction of these two idealized load factors gives rise to the critical load factor λ_c at temperature T, as follows:

$$1/\lambda_c(T) = 1/\lambda_p(T) + 1/\lambda_e(T) \qquad (4.1)$$

Alternatively, if the critical temperature T_c is of interest while the applied working loads remain constant, a trial-and-error procedure is necessary to determine T_c such that the sum of $1/\lambda_p(T)$ and $1/\lambda_e(T)$ is equal to unity. Clearly, at any $T<T_c$, the determined critical load factor is greater than unity. Thus, the frame remains safe under its working loads. However, when T is increased to T_c, the frame turns into a state of instability even under its working loads and partial or overall collapse may occur. ($\lambda_c(T)=1$)

The assumptions for Rankine approach that is extended to thermal effects are:

- Temperature distribution within a member is uniform
- Members are perfectly straight, isotropic and prismatic.
- Members buckle in the plane of the frame only.
- Local and lateral torsional buckling are not taken into account.
- Applied working loads are concentrated and proportional.

The elastic modulus E and the yield strength f_y are two dominant parameters in the Rankine approach. In the rigid-plastic analysis to determine λ_p, the steel stress-strain relationship is assumed to be perfectly plastic; in the elastic buckling analysis to determine λ_e, the steel stress-strain relationship is assumed to be linearly elastic. The variations of E and f_y with respect to elevated temperatures are assumed to comply with Eurocode 3 (EC3-Part1.2)

Additionally, according to Rankine formula there are two other important parameters governing the performance of a structure under fire conditions. These two parameters are the plastic load factor, λ_p, and the elastic buckling load factor, λ_e. A uniform temperature distribution within the members of the frame is assumed and a unique critical temperature is to be found with the help of these two parameters.

4.3. Second Order Analysis

In a first-order elastic analysis, equilibrium and kinematic relationships are based on the undeformed geometry of the structure. Solutions of these analyses are typically simple and straightforward. However, when lateral loads are applied to the structure, "it often assumes a configuration which deviates quite noticeably from its undeformed configuration," (Chen and Lui, 1991) requiring a second-order analysis. Chen and Lui report that a second-order analysis, which applies equilibrium and kinematic relationships to the deformed structure, "is always necessary for the stability consideration of structures" (1991). Since the deformation is unknown when the equilibrium and kinematic relationships are established, the second-order solution must be iterative, where the "deformed geometry of the structure obtained for a preceding cycle of calculations is used

as the basis for formulating the equilibrium and kinematic relationships for the current cycle of calculations" (Chen and Lui, 1991). Since the full consideration of second-order effects can be tedious and time-consuming and since exact solutions are not typically necessary, several simplified methods have been developed to approximate the second-order solution and make the analysis more efficient.

In general, the second-order effects on a frame are accounted for by a combination of P-Δ effects, which correspond to the frame, and P-δ effects, which correspond to individual members within the frame. Since both of these contribute to the deformation of the frame, it is important to consider their combined effect. The secondary effects cause the member to deform more and induce additional stresses in the member. As a result, they have a weakening or destabilizing effect on the structure. To ensure a safe design, these secondary effects must be considered in the design of frames.

The behaviour of moment resisting frames is more complex than the behaviour of individual members because of continuity and axial restraint and because fire induced elongations and rotations affect other areas of the building which are not subjected to heating. Therefore, it is important to consider the lateral deformations and the resulting P-Δ effects under fire condition as well.

In general, there are several simplified methods available for completing a second order analysis. One of the solution procedures which includes frame P-Δ effects is the solution by the 'Stiffness Matrix Method'. By the help of this method it is also possible to find the second order effects of the system under elevated temperatures. The influence of the temperature change in the structure can be taken into consideration whereas the second order effects are considered as well. By the help of the stiffness matrix method, it is possible to write the stiffness matrix of the system. Besides, load matrices which belong to the system can be written as well. The influence of the elevated temperature can be considered whereas the influence of the axial force effects is considered at the same time. The model which helps to derivate the stability functions equations is given in Figure 4.2. By the help of these equations of stability functions, the second-order effects under fire can be determined. The stiffness matrix and load vector of the elements of the system including

the second order effects are derived using the stability functions. The stability functions used in the analysis are given by the equations down below.

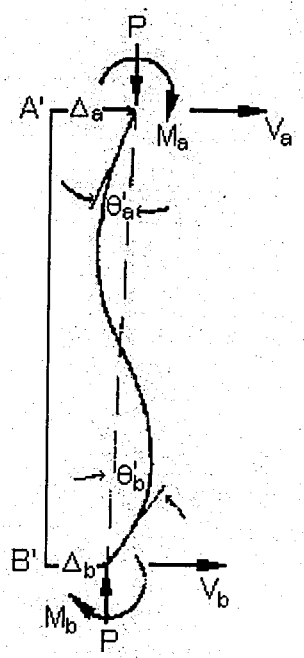

Figure 4.2. Flexural degrees of freedom, end forces and moments in X-Y plane

$$k = \sqrt{P/(E*I/L^2)} \tag{4.2}$$

$$e_i = e_j = \frac{k*L*(SinkL - kL*CoskL)}{4*\phi_c} \tag{4.3}$$

$$e_{ij} = \frac{k*L*(k*L - SinkL)}{2*\phi_c} \tag{4.4}$$

$$\phi_c = 2 - 2*CoskL - k*L*SinkL \tag{4.5}$$

k: Stability function in the X-Y plane

P: Applied axial load to the ends of the elements

E: Modulus of elasticity

I: Elements' moment of inertia

L: Elements' length

Φ_c: Stability function under compression

e_i, e_j, e_{ij}: Stability function coeficients of the stiffness matrix of the system

According to the equations above, the calssical stability equations under end compressive loads P in a single plane are formulated using the stiffness coefficients. Due to these equations, the stiffness matrix of the system changes due to the increment of the axial loads and the elevated temperature. Stability function coefficients change the sytem stiffness matrix and the load vectors. Therefore, the system has to be resolved when the affect of the second order effects are taken into consideration.

5. CASE STUDY 1: DESIGN OF PORTAL STEEL FRAME

5.1. Portal Frames

An alternative, economic solution to the design of a single story building is to use portal frame construction. Because of their clean lines, good overhead clearance and relatively low cost, portal frame buildings have become very popular. A large percentage of the small to medium size single-storey industrial buildings are made up in current use.

A very common form of steel construction is single storey portal frames. Steel portal frames are typically used as industrial building frames as shown in Figure 5.1; to support elevated machine components; and for overhead electrification of railway tracks in many countries. But while their use is being spread rapidly to the countries, the importance of the fire protection in the steel frames is usually being forgotten. The primary goal of the fire protection is to limit, to acceptable levels, the probability of death, injury and property of loss in an unwanted fire.

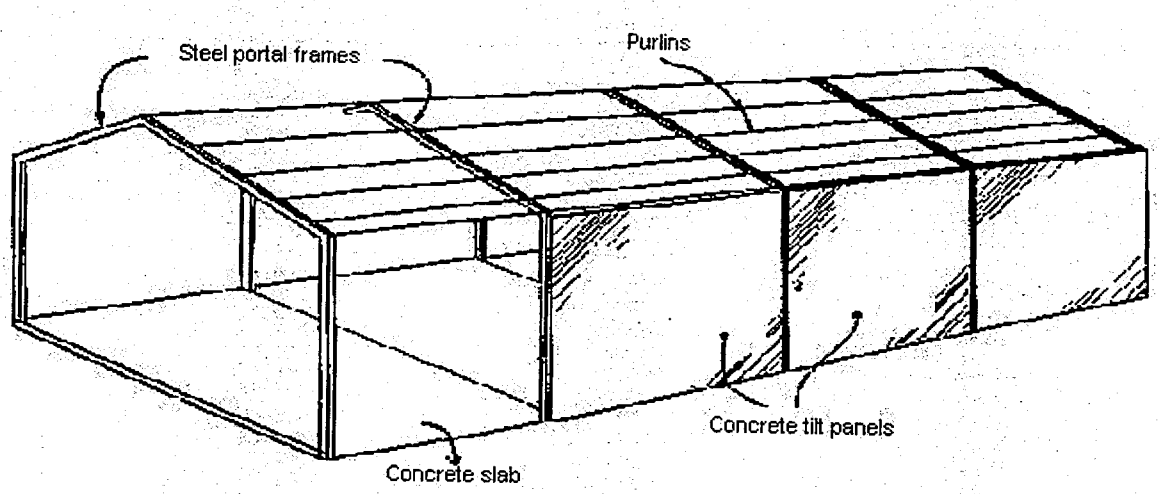

Figure 5.1. Single storey portal frame industrial building (Buchanan, 2000)

Portal frame construction has been widely based on the principles of plastic design. Additionally, the fire analysis of the steel portal frames is based on the plastic analysis as well.

5.2. Structural System

In this study, a frame which is a regular, one bay and one storey portal frame is modeled and designed in SAP2000 structural analysis program. Height of the system is 5 meters and horizontal dimensions of the system are 12 m by 40 m. The interior span is 4.6 m and the exterior span is 3.9 m in the frame system. Aluminum trapezoid plate is used as a lightweight roof cladding. A 3D view of the model is demonstrated in Figure 5.2 and structural members and dimensions are shown in Figure 5.3.

A portal frame is a type of steel structure which is composed of columns, beams and purlins. Construction materials used for the members are all steel. Steel type is Grade 43. Design strength of steel is $f_y = 275$ N/mm^2. Column sections are chosen as UC shape and beam and purlin sections are chosen as UB shape.

The structure is located in the first seismic zone and site class is chosen as Z4 according to the TEC-98 'Specification for Structures to be Built in Disaster Areas'.

5.3. Elastic Design of the Portal Frame

A portal frame structure is modeled and analyzed by using SAP2000 structural analysis program. The system is considered as a 2D frame in the analysis to have the exact solutions for the plane frame. The section of the beams is assigned according to the UB sections and the section of the columns is assigned according to the UC sections.

Dead, live, wind and earthquake loads are the considered loads acting on the frame system. These loads and their parameters were defined according to the provisions of TS 498 'Design Loads for Buildings'.

Dead loads consist of the weight of all materials of the structure incorporated into the building including roof cladding, connections and the unit weight of frame. In this study, unit weight of roof cladding (aluminum trapezoid plate) is 150 N/mm^2.

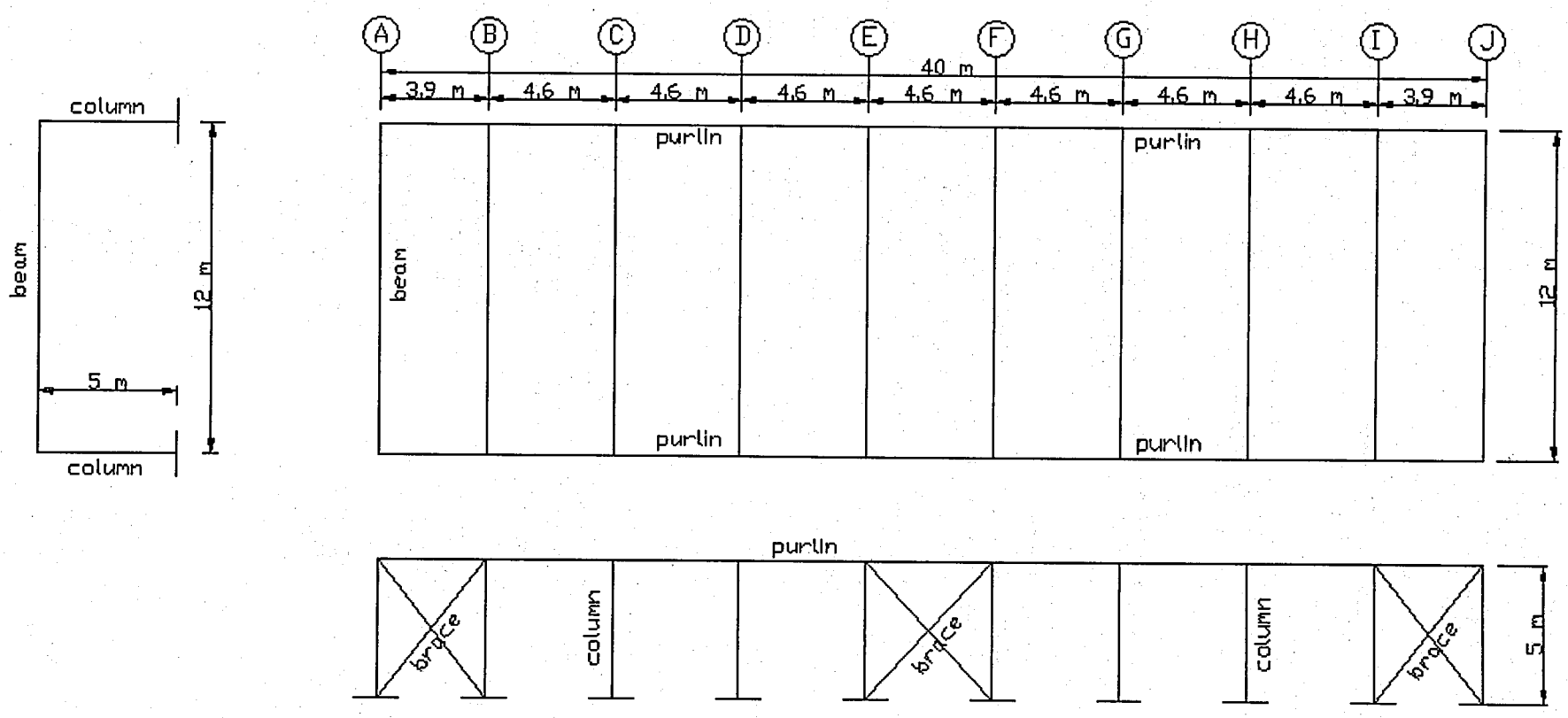

Figure 5.3. Structural members and dimensions of the system

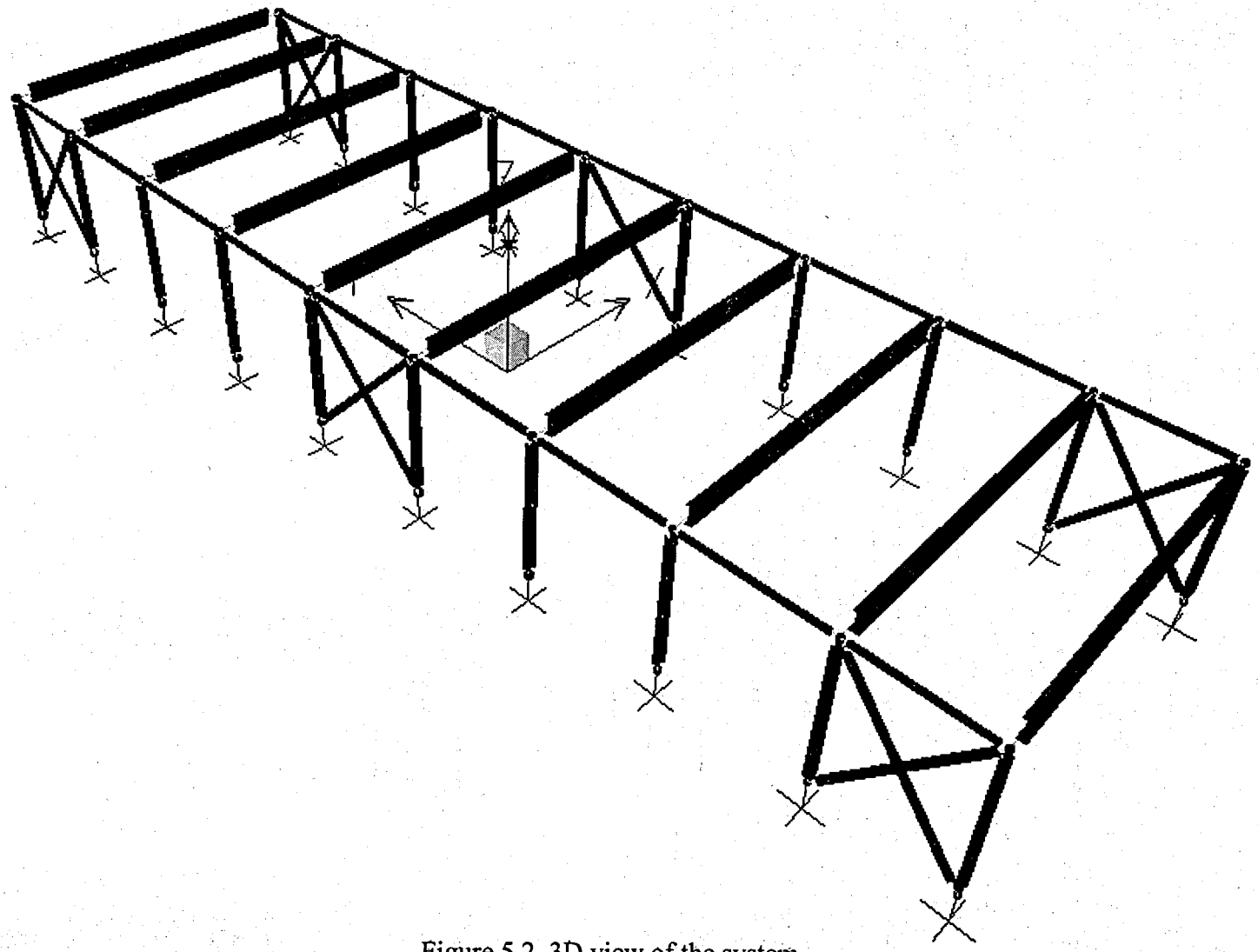

Figure 5.2. 3D view of the system

Live loads do not include construction and environmental loads such as earthquake loads, wind loads or dead loads. Live loads are produced by the use and occupancy of the building or the other structures in TS 498. According to TS 498, live load is taken as 1.5 kN/m^2.

Wind loads acting on the structure are obtained according to the provision of TS 498. Wind load depends on the geometry of the structure and also consider the pressure, absorption and friction effects in the calculation. Wind pressure, q, is defined according to the height of the structure from the ground. According to TS 498, if the height of the structure is between 0 and 8 m then wind pressure for the structure is taken as 0.5 kN/m^2. Schematic of the wind load on a steel portal frame is shown in Figure 5.4.

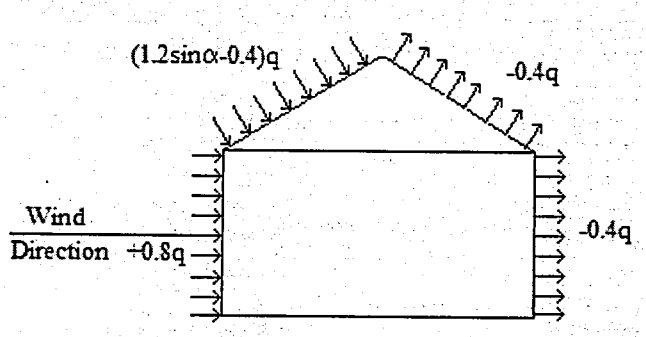

Figure 5.4. Schematic of the wind load

Earthquake loads on a structure depend on the properties of the structure itself, seismic properties and soil type of the site where the structure is built up. Earthquake loads are obtained according to the provisions of TEC-98. The structure is located in the first seismic zone. Therefore, ground acceleration coefficient, A_0, is 0.4 and the chosen site class is Z4. So, spectrum characteristic periods which are T_A and T_B, are 0.2 sec and 0.9 sec, respectively. Occupancy importance factor, I, is taken as 1.5 and response modification factor, R, is taken as 8 in calculations.

Equivalent earthquake method which is mentioned in TEC-98 is used for determining the earthquake force. The first natural period of the system is calculated by the formula (TEC-98) given in Equation 5.1;

$$T_1 \cong T_{1A} = C_t H_N^{3/4} \tag{5.1}$$

where, T_1 is the natural period of vibration, T_{1A} is the natural period of vibration calculated by empirical formula, C_t is the coefficient used in obtaining the first natural period of vibration which is taken as 0.08 for the steel frames and H_n is the total height of the system which is 5 m in the considered structure.

According to the information above, first natural period of vibration is calculated as 0.27 sec. Due to this calculated period, earthquake forces are found by the formula (TEC-98);

$$V_t = \frac{W * A(T)}{R} \tag{5.2}$$

where, V_t is the equivalent earthquake force, W is the total mass of the structure which is 187.2 kN, A(T) is the spectral acceleration coefficient which is calculated by the Equation 5.3 (TEC-98), R is the response modification factor which is taken as 8.

$$A(T) = A_0 * I * S(T) \tag{5.3}$$

In Equation 5.3, A_0 is the ground acceleration coefficient which is 0.4 in calculations, I is the occupancy importance factor which is 1.5 and S(T) is the spectrum coefficient which is found 2.5. According to the solution of this equation, 1.5 is found as the value of A(T). Due to the found value for A(T), Equation 5.2 is solved and the equivalent earthquake force V_t is found as 35.1 kN.

The load combinations and the load factors are obtained for the analysis and the design of the system. According to the TS 500 'Requirements for Design and Construction of Reinforced Concrete Structures' and TEC-98, the load combinations are defined in the analysis and the design of the structure is given below;

- 1.4 G + 1.6 Q
- G + Q + E_x

- $G + Q - E_x$
- $0.9\,G + E_x$
- $0.9\,G - E_x$
- $G + 1.3\,Q + 1.3\,W$
- $0.9\,G + 1.3\,W$

where,

G = Dead Load

Q = Live Load

E_x = Earthquake load in x-direction

W = Wind Load

By running SAP2000 structural analysis program, the system is analyzed according to the load combinations. Also, the structural frames are designed under unfavorable load combination which is 1.4 G + 1.6 Q load combination. The design section of columns and beams are checked according to the provisions of BS 5950 'British Standard Institute' whether they are in the limit or not. According to the elastic analysis result, the sections have been chosen from universal beam sections as UB 305*165*40 for the beams and universal column sections as UC 203*203*52 for the columns. Section properties are shown below in Table 5.1.

Table 5.1. Section properties due to elastic analysis

Section	G (kg/m)	A (cm^2)	I_y (cm^4)	I_z (cm^4)	$W_{el,y}$ (cm^3)	$W_{el,z}$ (cm^3)
UB 305*165*40	40.3	51.32	8503	764.4	623.1	92.65
UC 203*203*52	52	66.28	5259	510.1	1778	174

In Table 5.1, G is the unit weight of the section. A is the cross sectional area. I_y is the strong axes moments of inertia and I_z is the weak axes moments of inertia. $W_{el,y}$ is the strong axes elastic modulus and $W_{el,z}$ is the weak axes elastic modulus.

The elastic design results are shown by the help of the graphs down below. Figure 5.5 shows the axial force distribution on the system, Figure 5.6 shows the shear forces acting on the system and finally Figure 5.7 shows the moment distribution of the system. These diagrams are plotted easily by the help of SAP2000 program.

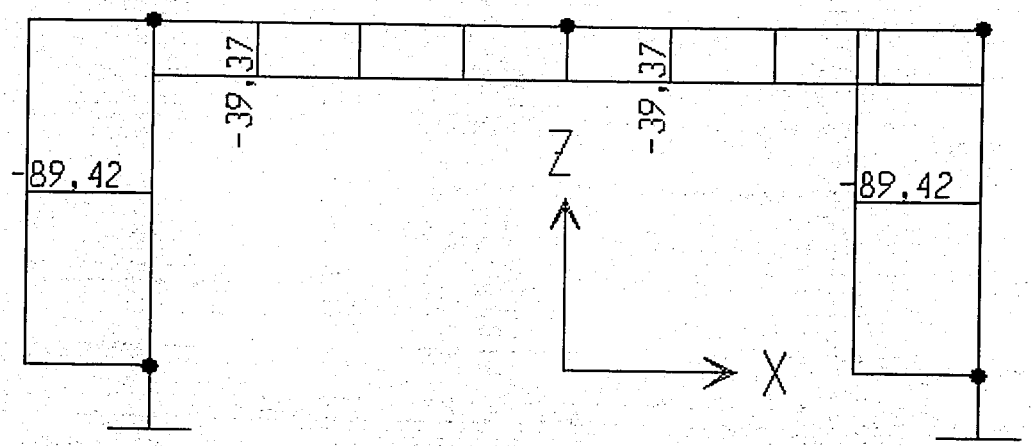

Figure 5.5. Axial force distribution of the system

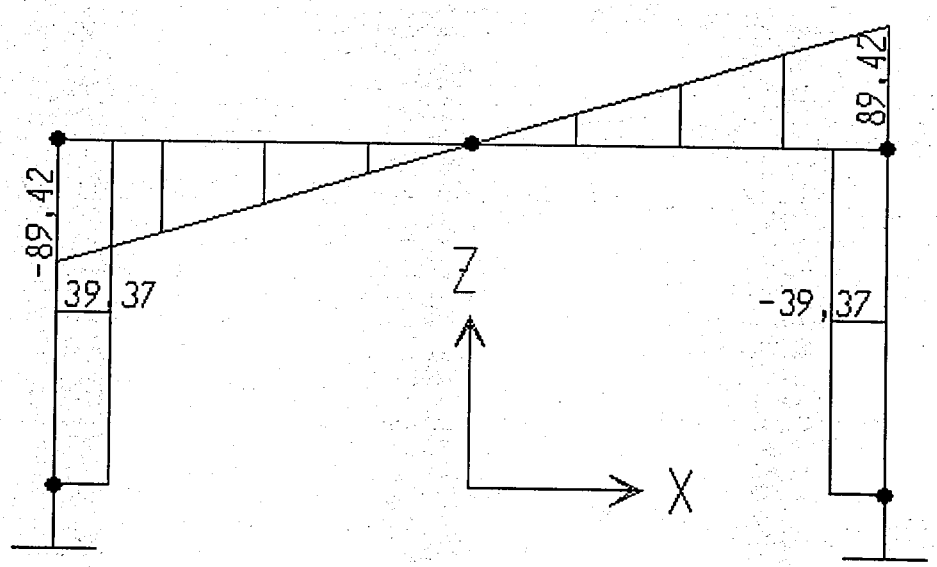

Figure 5.6. Shear force distribution of the system

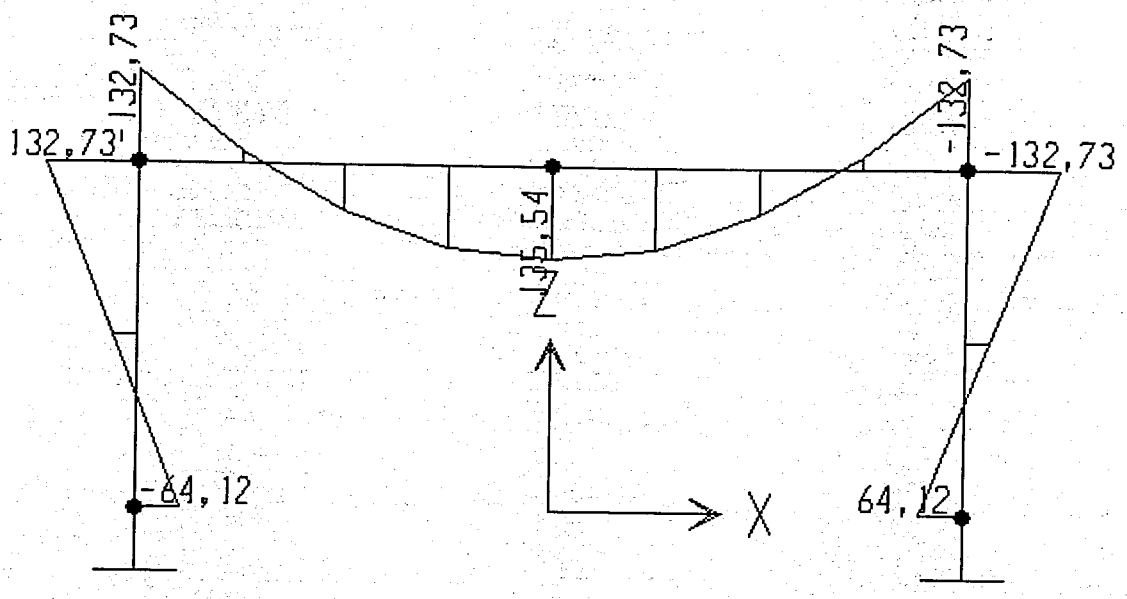

Figure 5.7. Moment distribution of the system

5.3.1. Design Checks According to the Provisions of BS 5950

The column is a uniform member subjected to axial load and moment. In column design, applied load F is 89.42 kN. For determining the in-plane effective lengths for portal members, Fraser's formula is used. According to Fraser's formula;

$$L_E / L = 2 + 0.45 * G_r \quad \text{and} \quad G_r = (L_b * I_c)/(I_b * L_c) \tag{5.4}$$

where, L_b and L_c are beam and column lengths.

Therefore, from Equation 5.4, $L_E / L = 2.21$.

Slenderness, λ, should be taken as the effective, L_E, divided by the radius of gyration about the relevant axis.

Slenderness in major axis,

$$\frac{L_{EX}}{r_x} = \frac{L_E}{L} * \frac{L_c}{r_x} = 2.21 * \frac{500}{8.91} = 124.01 < 180.$$ It is satisfied.

Slenderness in minor axis, $\frac{L_{EY}}{r_y} = \frac{(L_c/2)}{r_y} = \frac{(500/2)}{5.18} = 48.26$

$\frac{L_{EX}}{r_x} = 124.01 > \frac{L_{EY}}{r_y} = 48.26$. It is satisfied.

The compressive resistance, P_c, of a member should be obtained from the equation:

$$P_c = A_g * p_c \quad (5.5)$$

where, A_g is the gross sectional area and p_c is the compressive strength which is obtained from Table 27(a) in BS 5950 as 112 N/mm^2. The compressive resistance is computed as 742.34 kN.

Moment capacity, M_c, of a section can be obtained from the Equation 5.6;

$$M_c = p_y * S \quad (5.6)$$

where, p_y is the design strength and S is the plastic modulus of a section. M_c is computed as 156.03 kNm.

Buckling resistance, M_b, is given by:

$$M_b = p_b * S \quad (5.7)$$

where, p_b is the bending strength is related to the equivalent slenderness, λ_{LT}, the design strength of material, p_y. Bending strength can be obtained from Table 11 in BS 5950 code.

$$\lambda_{LT} = n*u*v*\lambda \quad (5.8)$$

In Equation 5.8,

n is the slenderness correction factor which is considered as 1

u is the buckling parameter of a section which is taken as 0.848

λ is the minor axis slenderness which is equal to 48.26

v is the slenderness factor which is obtained 0.91

According to these values, equivalent slenderness, λ_{LT}, is computed as 37.24. Bending strength, p_b, is read from Table 11 as 269 N/mm^2 in BS 5950 code.

From Equation 5.6, buckling resistance is computed as 152.63 kNm.

Equivalent uniform moment factor, m, is obtained from Table 18 in BS5950 code for β=-0.5 as 0.43.

Local capacity check:

$$\frac{F}{A_g p_y} + \frac{M_x}{M_c} = 0.899 \leq 1 \tag{5.9}$$

Local capacity check is satisfied.

Overall buckling check:

$$\frac{F}{A_g p_c} + \frac{m * M_x}{M_b} = 0.495 \leq 1 \tag{5.10}$$

Overall buckling check is satisfied.

The beam is subjected to bending. Maximum moment at mid-span is 35.54 kNm. and shear force, F_v, is 89.42 kN.

Shear control F_v is not greater than shear capacity, P_v. Shear capacity is given by:

$$P_v = 0.6 * p_y * A_v \tag{5.11}$$

where, p_y is the design strength and A_v is the shear area taken as:

$$A_v = t*D \tag{5.12}$$

where, t is the total web thickness which is taken as 6 mm and D is the depth which is taken as 303.4 mm. From Equation 5.12, shear area, A_v, is calculated as $1.82*10^{-3}$ m^2.

Shear capacity of a section is computed as 300.4 kN. Therefore, $F_v < P_v$ is satisfied.

If $F_v \leq 0.6P_v$, then the moment capacity, M_c, should be taken as Equation 5.6. According to Equation 5.6, moment capacity of a section is calculated as 171.35 kNm. This value is greater than the value of support and mid-span moment, so it is satisfied.

For members between adjacent lateral restraint, subjected to bending about their major axis the following condition should be satisfied:

$$\bar{M} \leq M_b \tag{5.13}$$

where, $\bar{M}$ is the equivalent uniform moment and M_b is the lateral torsional buckling moment.

Equivalent uniform moment is given by:

$$\bar{M} = m*M_A \tag{5.14}$$

where, M_A is the maximum moment on the member under consideration and m is an equivalent uniform moment factor which is considered as 1 according to Table 18 in the provision of BS 5950 code. According to Equation 5.14, equivalent uniform moment is calculated as 132.73 kN.

Buckling resistance, M_b, can be calculated by using Equation 5.7. Equivalent slenderness, λ_{LT}, is computed as 55.26. Bending strength, p_b, is read from Table 11 as 226

N/mm^2 in BS 5950 code. By using Equation 5.7, buckling resistance, M_b, is computed as 140.8 kNm. According to the equivalent uniform moment and buckling resistance, Equation 5.14 is satisfied.

5.4. Plastic Design of the Portal Frame

The plastic methods of structural analysis are now widely used in the design of steel frames. For such structures, the most economical design is achieved by the use of the plastic methods.

In this study, semi-graphic static method is used for the application of the plastic method. This method is particularly well suited for the treatment of rectangular or gabled pinned-base frames of one or several bays. It is shown in Figure 5.8. It is important to note that the value of the plastic moment capacity has been determined for a rigid-jointed plane frame without requiring any prior knowledge of section properties, unlike elastic design. The procedure of this method is detailed in the following;

- The system's redundancies which must form a complete set in the sense that the structure becomes statically determinate when all the redundancies are given the value zero are chosen.
- The primary structure's bending moment diagram which is called 'Statically Determinate Bending Moment Diagram' is drawn.
- 'Statically Indeterminate Bending Moment Diagram' which corresponds to unspecified values of the redundancies is sketched.
- 'Actual Bending Moment Diagram' is constructed by the superposition of the diagrams under the statically determinate bending moment diagram and above the statically indeterminate bending moment diagram. The values of the redundancies are drawn to satisfy the magnitude of the actual bending moment not to exceed the plastic moment and to satisfy the insertion of the hinges at the sections to transform the structure into a mechanism at which the magnitude of the actual bending moment equals the plastic moment.

- A deformation of this mechanism for which the total work done by the loads is positive is sketched to check whether the signs of the relative rotations in the plastic hinges agree with the signs of the actual bending moments at the hinge sections.

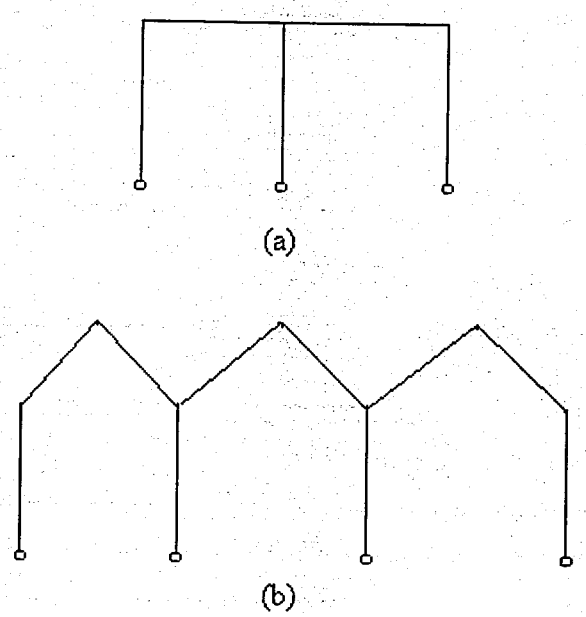

Figure 5.8. Rectangular and gable pinned-base portal frame of several bays (Massonet and Save, 1965)

The load combination in the design of the system for the plastic analysis is given below;

- 1.4 G + 1.6 Q
- G + 1.3 Q + 1.3 W
- 0.9 G + 1.3 W

5.4.1. Plastic Analysis under 1.4 G + 1.6 Q Load Combination

The first plastic analysis is done under the load combination of 1.4 G + 1.6 Q which is composed of dead and live loads. A dead load of 2.76 kN/m and a live load of 6.9 kN/m are uniformly distributed on the beam of the frame. Therefore, the total load acting on the frame according to the 1.4 G + 1.6 Q combination is 14.9 kN/m. Uniformly distributed load and the geometry of the frame are shown below in Figure 5.9.

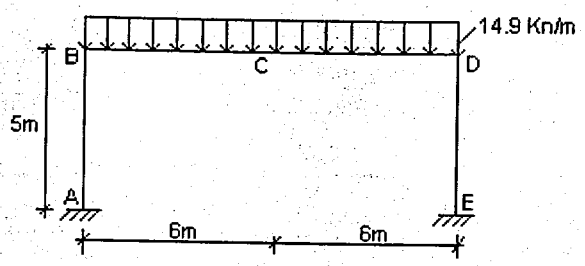

Figure 5.9. Geometry and load distribution of 1.4 G + 1.6 Q for the portal frame

To start the plastic analysis, a free bending moment diagram must be drawn and the reactant line positioned to give collapse by one or other of the modes. Alternatively, the work balance equations must be written for each of the modes. The solution giving the highest value of M_p is the correct solution.

To be able to draw the free bending moment diagram, the frame must be made statically determinate. The best way of making the frame determinate is to divide the frame into two from the apex. As it is given in the Figure 5.10, the dead and live loads on the portal frame are symmetrical about the centerline. Therefore, the work involved in calculating bending moments is reduced by cutting the frame in this way.

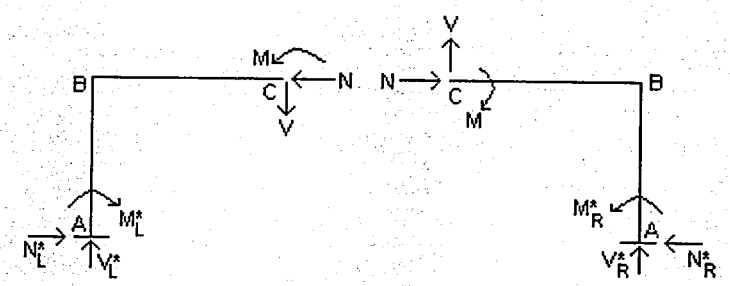

Figure 5.10. The geometry of free and reactant moment diagrams

The equations belong to the Figure 5.10 are given below;

$$M_L^* = M + 5*N - 6*V \tag{5.15}$$

$$M_R^* = M + 5*N + 6*V \tag{5.16}$$

where,

M^*_L: Moment on the left fixed end

M^*_R: Moment on the right fixed end

N^*_L, V^*_L: Fixed end reactions on the left

N^*_R, V^*_R: Fixed end reactions on the right

The uniform vertical load combination has been split into two equal parts. There is no virtue in this equal division beyond that of preserving symmetry, since the correct answer will be derived from any other division. After this, the free bending diagram which is shown in Figure 5.11 is now easily drawn. From Figure 5.11, it is seen that the portal frame has been opened out into a straight line consists of points named A, B, C, D, E.

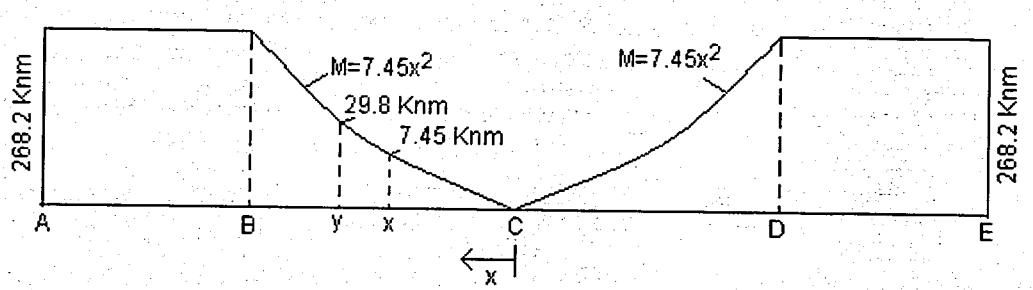

Figure 5.11. Free moment diagram for the portal frame

The portal frame design here is governed by the gravity loading. By applying plastic design principles and general expressions for the plastic moment capacity M_p of a uniform frame can be derived for the fixed end conditions. It is assumed that the distance between the purlins is 1 m in horizontal. X, Y etc. symbolizes the places of the purlin points.

The reactant diagram may be constructed by considering the effect of the redundant actions destroyed by cutting the frame into two. These redundancies are shown in Figure 5.10 as a moment M and two forces N and V. Then they are lead to the diagram shown as Figure 5.12. In this figure, the slopes of the reactant lines for AB and DE are equal and opposite because of the symmetry. Also, the shape of the frame is thus reproduced to some extent in the reactant diagram.

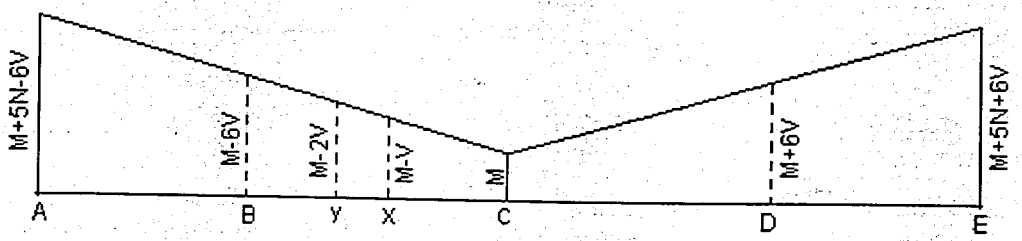

Figure 5.12. Reactant moment diagram for the portal frame

For achieving the total bending moment diagram for the portal frame, Figure 5.11 and 5.12 must be superimposed. Figure 5.13 shows the superimposed diagram which gives the net moment values. According to this achieved diagram, it is first supposed that the collapse occurs by the hinge at B, X, D and E. Due to the situation, simultaneous equations can be written.

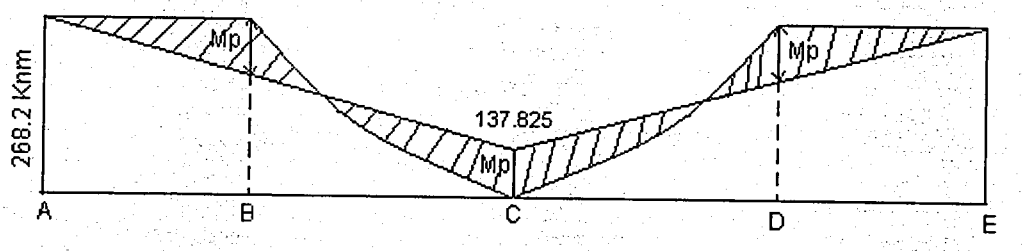

Figure 5.13. Net moment diagram for the portal frame

At B: $268.2 - (M - 6*V) = M_p$ (5.17)

At X: $7.45 - (M - V) = -Mp$ (5.18)

At D: $268.2 - (M + 6V) = Mp$ (5.19)

At E: $268.2 - (M + 5*N + 6*V) = 0$ (5.20)

First, it is considered that the hinge might occur on the X point. By solving these equations according to that, it is seen that the plastic moment of column ($M_{p,\ column}$) is 130.375 kNm and is smaller than the moment M which is 137.825 kNm. The result of the equations, $M > M_{p,\ column}$ can not be accepted. Therefore, the plastic hinge is assumed to be on point C and the purlin distance is taken zero. When the equations are solved again according to this, the plastic moment of column ($M_{p,\ column}$) is 134.10 kNm and the plastic moment of the beam ($M_{p,\ beam}$) is 100.575 kNm. The horizontal reaction N is 26.82 kN. In

this case, it is seen that $M \leq M_{p,\,column}$ which is required. The assumed hinge positions are checked to see if they are correct or not as well.

As a result of this, because of the results achieved from the equations, it is seen that the hinge forms at point C for the first load combination which is 1.4 G + 1.6 Q.

5.4.2. Plastic Analysis under G + 1.3 Q + 1.3 W Load Combination

The second plastic analysis is done under the load combination of G + 1.3 Q + 1.3 W which is composed of dead, live and wind loads. A dead load of 2.76 kN/m and a live load of 6.9 kN/m are uniformly distributed on the beam of the frame. Also, the wind load is acting on the sides of the frame which is, W_{left}, 1.84 kN/m on the left side and W_{right}, 0.92 kN/m on the right side. Therefore, the total load acting on the beam according to this load combination is G + 1.3 Q which is 11.73 kN/m and the load acting on the columns is the 1.3 W_{left} and 1.3 W_{right} which are 2.392 kN/m and 1.196 kN/m, respectively. Uniformly distributed loads and the geometry of the frame are shown below in Figure 5.14.

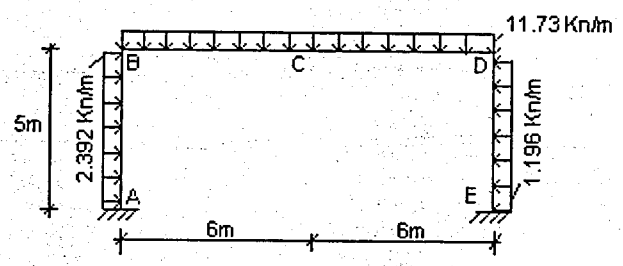

Figure 5.14. Geometry and load distribution of G + 1.3 Q + 1.3 W for the portal frame

A free bending moment diagram of the system has to be drawn to start the plastic analysis here, too. To be able to draw the diagram easily, the diagram for the G + 1.3 Q and the diagram for the 1.3 W combinations are drawn separately and then superimposed. The free bending diagrams due to these load combinations are shown in Figure 5.15 and 5.16.

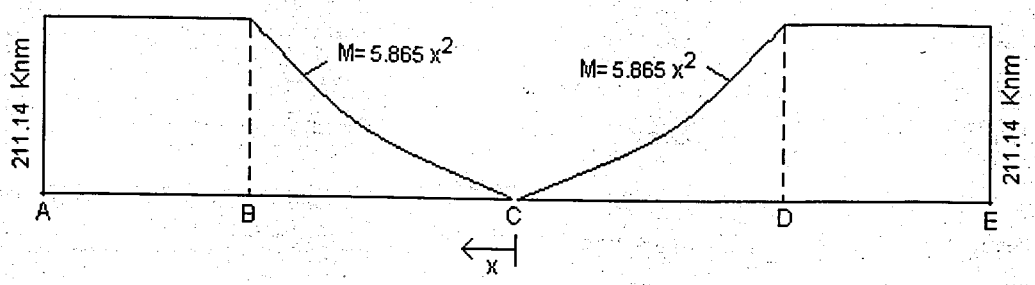

Figure 5.15. Free moment diagram due to G + 1.3 Q load combination

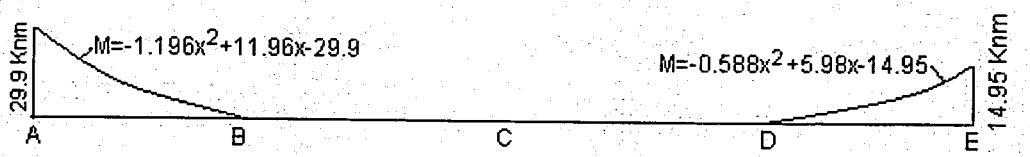

Figure 5.16. Free moment diagram due to 1.3 W load combination

The reactant diagram may be constructed by the same way followed in the first load combination. After it is drawn, the reactant diagram has to be superimposed with the free moment diagrams shown in Figure 5.15 and 5.16 to achieve the net moment diagram for the second load combination. The net moment diagram which will help to write the equations is shown below in Figure 5.17.

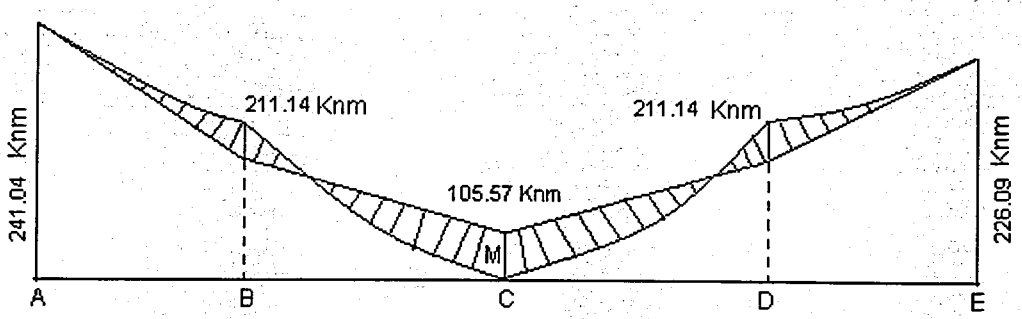

Figure 5.17. Net moment diagram for the load combination G + 1.3 Q + 1.3 W

At B: $211.14 - (M - 6*V) = M_p$ (5.21)

At X: $5.865 - (M - V) = -M_p$ (5.22)

At D: $211.14 - (M + 6*V) = M_p$ (5.23)

This time, by solving these equations according to the consideration of plastic hinge on X, it is seen that the plastic moment of column ($M_{p,\,column}$) is 102.64 kNm and is smaller than the moment M which is 108.5 kNm. The result of the equations, $M > M_{p,\,column}$ can not be accepted again. Therefore, the plastic hinge is assumed to be on point C and the purlin distance is taken zero once again. When the equations are solved again according to this consideration, the plastic moment of column ($M_{p,\,column}$) is 105.57 kNm and the plastic moment of the beam ($M_{p,\,beam}$) is 79.18 kNm. In this case, it is seen that $M \leq M_{p,\,column}$ which is required. The assumed hinge positions are checked again to see if they are correct or not as well.

As a result of this, because of the results achieved from the equations, it is seen that the hinge forms at point C for the second load combination which is G + 1.3 Q + 1.3 W.

5.4.3. Plastic Analysis under 0.9 G + 1.3 W Load Combination

The third plastic analysis is done under the load combination of 0.9 G + 1.3 W which is composed of dead and wind loads. A dead load of 2.76 kN/m is uniformly distributed on the beam of the frame. Also, the wind load is acting on the sides of the frame which is, W_{left}, 1.84 kN/m on the left side and W_{right}, 0.92 kN/m on the right side. Therefore, the total load acting on the beam according to this load combination is 0.9 G which is 2.48 kN/m and the load acting on the columns is the 1.3 W_{left} and 1.3 W_{right} which are 2.392 kN/m and 1.196 kN/m, respectively. Uniformly distributed loads and the geometry of the frame are shown below in Figure 5.18.

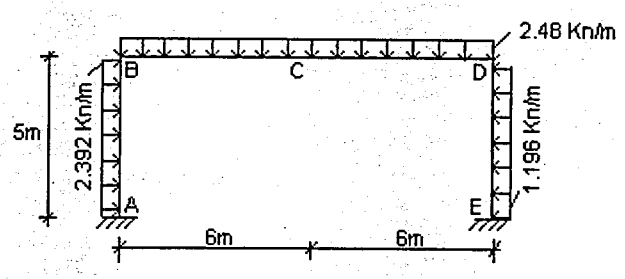

Figure 5.18. Geometry and load distribution of 0.9 G + 1.3 W for the portal frame

For drawing the free moment diagram of the portal frame, the load combination is divided into two. Therefore, free moment diagram for the loads acting on the beam which

is 0.9 G and free moment diagram for the loads acting on the columns which is 1.3 W are drawn separately and shown in the figures below. Figure 5.19 shows the free moment diagram due to the 0.9 G load combination and Figure 5.20 shows the free moment diagram due to the 1.3 W load combinations. Afterwards, these two diagrams are superimposed.

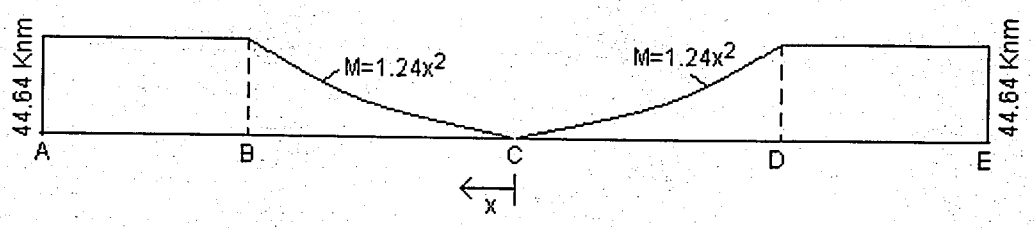

Figure 5.19. Free moment diagram due to 0.9 G load combination

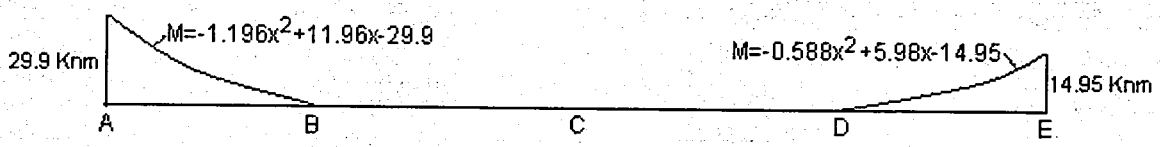

Figure 5.20. Free moment diagram due to 1.3 W load combination

The reactant moment diagram may be constructed by the same way followed in the first two load combinations. After the reactant moment diagram for the 0.9 G + 1.3 W load combination is drawn, this moment diagram has to be superimposed with the free moment diagrams shown in Figure 5.19 and 5.20 to achieve the net moment diagram for the third load combination.

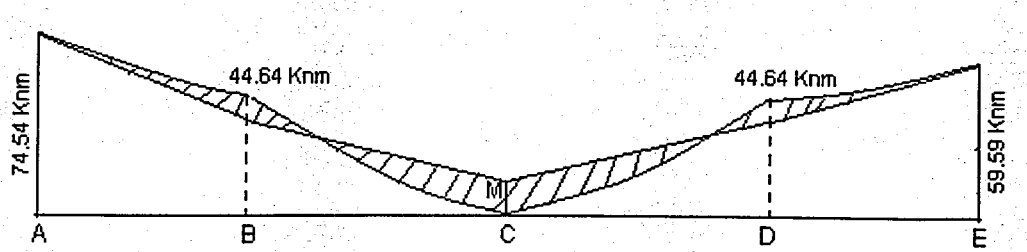

Figure 5.21. Net moment diagram for the load combination 0.9 G + 1.3 W

The net moment diagram is shown in Figure 5.21. By the help of the net moment diagram, the equations for the plastic analysis are written, as well.

$$\text{At B: } 44.64 - (M - 6*V) = M_p \quad (5.24)$$

$$\text{At X: } 0.31 - (M - V) = -M_p \quad (5.25)$$

$$\text{At D: } 44.64 - (M + 6*V) = M_p \quad (5.26)$$

The solution procedure followed for the other load combinations are valid in this load combination as well. For the 0.9 G + 1.3 W load combination, by solving these equations starting with the consideration of plastic hinge on X, it is observed that the plastic moment of column ($M_{p,\ column}$) is 22.165 kNm and is smaller than the moment M which is 22.475 kNm. The result of the equations, $M > M_{p,\ column}$ can not be accepted again in this situation. Therefore, the plastic hinge is carried to point C and the purlin distance is taken zero once again. When the equations are solved again according to this consideration, the plastic moment of column ($M_{p,\ column}$) is 22.32 kNm and the plastic moment of the beam ($M_{p,\ beam}$) is 16.74 kNm. In this case, it is seen that $M \leq M_{p,\ column}$ which is required. The assumed hinge positions are checked again to see if they are correct or not as well.

As a result of this, because of the results achieved from the equations, it is once again seen that the hinge forms at point C for the third load combination which is 0.9 G + 1.3 W.

According to the plastic analysis done for the three load combinations, it is seen that the mechanism is formed under the first load combination which is 1.4 G + 1.6 Q. The first load combination gives the highest M_p value for the beams and the columns when it is compared with the other load combinations applied to the portal frame. According to this M_p value which is 134.10 kNm for the plastic moment of columns ($M_{p,\ column}$) and 100.575 kNm for the plastic moment of beams ($M_{p,\ beam}$), proper sections are chosen for the portal frame. The plastic modules of the sections are found due to the Equation 5.27 in the next page by the help of the M_p values to choose the correct section sizes. Afterwards, according to the material properties of steel, the sections are found from the 'British Universal Beams and Columns Tables'.

$$M_p = W^* \sigma_{yield} \quad (5.27)$$

Table 5.2. Section properties due to plastic analysis

Section	G (kg/m)	A (cm^2)	I_y (cm^4)	I_z (cm^4)	$W_{pl,y}$ (cm^3)	$W_{pl,z}$ (cm^3)
UB 254*146*31	31.10	39.68	4413	447.5	393.10	94.13
UC 203*203*46	46.10	58.73	4568	1548	497.40	230.90

5.4.4. Sway Stability of Portal Frame

In the plastic design of portal frame attention should be paid to the deflection of the frame at serviceability loading. In the absence of a rigorous analysis of frame stability the following condition should be satisfied.

The horizontal deflection, δ, calculated by linear elastic analysis at the top of any column due to the notional horizontal loading should not exceed h/1000, where h is the height of the column. The horizontal deflection, δ, is obtained as 2.33E-04 from the analysis and it satisfied the condition $\delta \leq (h/1000) = 0.005$.

In calculating δ allowance may be made for the restraining effect of cladding.

$$\frac{L}{D} \leq \frac{44}{\Omega} \frac{L}{h} \frac{\rho}{(4 + \rho L_r / L)} \frac{275}{p_{yr}} \quad (5.28)$$

$$\rho = \frac{2I_c}{I_r} \frac{L}{h} \qquad \text{for single-bay portal frame} \quad (5.29)$$

where;

L = span of the bay

D = min. depth of the beam

h = column height

I_c = min. second moment area of the column

I_r = min second moment area of the beam

L_r = total developed length of the beam

Ω = arching ratio defined as W_r/W_0

W_r = factored vertical load on the beam

W_0 = max. value of the beam treated as a fixed ended beam of span L

From Equation 5.29, p is calculated as 16.60.

From Equation 5.28,

$$\frac{12}{0.251} = 47.80 \leq \frac{44}{1} * \frac{12}{5} * (\frac{16.60}{4+16.60*1}) * (\frac{275}{275}) = 85.09$$

Therefore frame is stable.

The plastic design produces lighter and more slender structural proportions than similar frames designed by elastic theory. As it is seen from the Table 5.3, plastic design sections are lighter in this study as well. The beam and column sections are 20% lighter in plastic analysis. When the sections found in the plastic analysis are compared with the sections found in the elastic analysis, it is seen that the sections' properties are close to each other for each element and that the plastic sections are more economical than the elastic sections. Therefore, plastic design is more economic solution than the elastic design. This comparison between the elastic sections and the plastic sections are showed in Table 5.3.

Table 5.3. Comparison of the sections according to the elastic and plastic design

	Elastic Design	Plastic Design
Column section	UC 203*203*52	UC 203*203*46
Beam section	UB 305*165*40	UB 254*146*31
Weight of column section (kg/m)	52.00	46.10
Weight of beam section (kg/m)	40.30	31.10

6. CASE STUDY 2: ANALYSIS OF STEEL FRAMES UNDER FIRE

6.1. Design Values at Elevated Temperatures

For design purposes, many national codes have proposed slightly different approximations to the published test data. The parameters needed for the calculations have to be considered under elevated temperature. Typical relationships in yield strength and modulus of elasticity with temperature are shown in Figure 6.1 which is reproduced from the Eurocode 3 (EC3, 1995). The reduction in yield strength, proportional limit and modulus of elasticity are defined by a number of points.

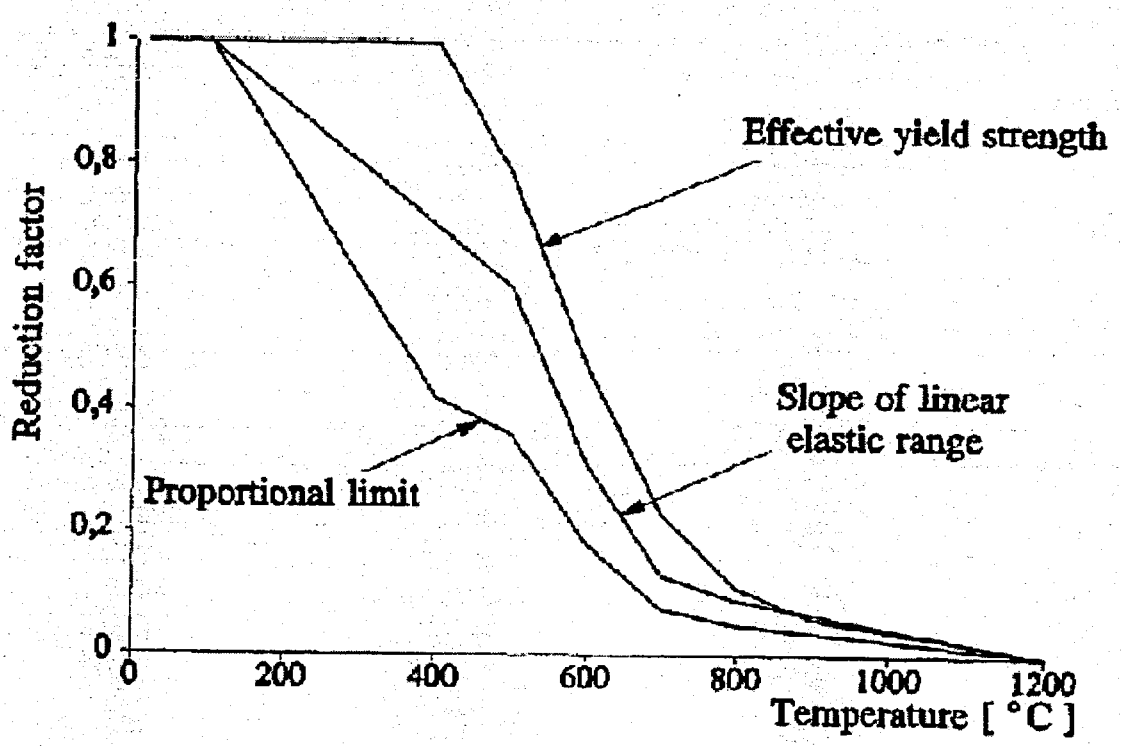

Figure 6.1. Reduction factors for the stress-strain relationship of steel at elevated temperature

According to this, the equation for the yield strength of structural steel at elevated temperature is given with Equation 6.1;

$$k_{y,T} = (905\text{-}T) / 690 \qquad (6.1)$$

where, $k_{y,T}$ is the ratio of $f_{y,T}$ (the yield strength at elevated temperature) to f_y (the yield strength at 20°C).

The relationship in Equation 6.1 can be reversed to give the limiting temperature for a given load ratio. The limiting temperature is that at which an individual steel member is expected to fail, assuming no load sharing or redundant behaviour. The limiting temperatures which are critical temperatures are given by the Equation 6.2 below;

$$T_c = 905 - 690*R \tag{6.2}$$

where, R is the load ratio.

The modulus of elasticity is another parameter changing by the increase and decrease of the temperature. Therefore, the value of the modulus of elasticity must be considered under elevated temperature as well. The modulus of elasticity is needed for buckling calculations. It would also be required for elastic deflection calculations but these are rarely attempted under fire conditions because elevated temperatures lead rapidly to plastic deformations. The reduction in modulus of elasticity shows the same trend as the reduction in yield strength. There can be obvious numerical difficulties if both properties do not reach zero at the same temperature. The Eurocode 3 (EC3, 1995) reduction in modulus of elasticity with temperature is shown in Figure 6.1. According to that, the modulus of elasticity of the structural steel at elevated temperature is given with Equation 6.3 and Equation 6.4;

$$k_{E,T} = 1.0 + T / [2000*\ln(T/1100)] \qquad 0<T\leq 600°C \tag{6.3}$$

$$k_{E,T} = 690*(1 - T/1000) / (T-53.5) \qquad 600<T\leq 1000°C \tag{6.4}$$

where, $k_{E,T}$ is the ratio of E_T (the modulus of elasticity at elevated temperature) to E (the modulus of elasticity at 20°C).

According to all these changes in the parameters due to the elevated temperature, the calculations can be done correctly by considering the change in the values.

6.2. Design Procedure at Elevated Temperatures

The present work will deal with two accepted methods; one the empirical Rankine Approach, the other Upper Bound Approach. The methods are aiming to obtain a critical temperature, the temperature at collapse conditions, of framed structures under elevated temperatures. The safety of the example steel portal frame is to be checked against collapse load factors as well.

From the plastic analysis, it is seen that the beam mechanism has given the highest M_p values. According to this result, the beam mechanism will be taken in the fire analysis. Therefore, the model to be analyzed with the determined approaches is as it is in the Figure 6.2. The columns are UC 203*203*46 whereas the beam of the portal frame is UB 254*146*31. The yield strength, f_y, at ambient temperature of these materials is 275000 kN/m^2.

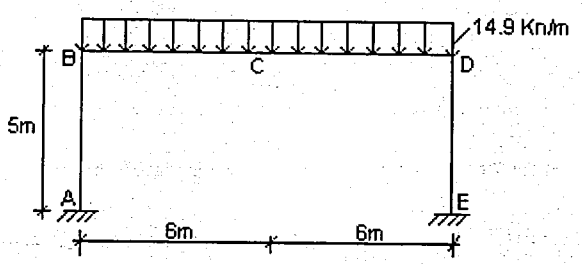

Figure 6.2. The portal frame model used in analysis

To start the analysis for the steel frame under fire, the plastic moment capacities at elevated temperature must be found. Therefore, the beam and the columns are considered separately and their section parameters and plastic moment capacities are found at elevated temperatures.

6.2.1. Analysis of the Beams Subjected to Four Sided Exposure to Fire

The strength of the beams belongs to the portal frame under fire conditions can be determined as follows shown in the equations given in the next page starting with the Equation 6.5;

$$M_{PT} = S * f_{y,T} \tag{6.5}$$

where,

M_{PT} = The plastic moment capacity at given elevated temperature

S = The plastic section modulus

$f_{y,T}$ = The yield stress at given elevated temperature

The relationship between the temperature and the yield stress ratio is given by the Equation 6.6.

$$\frac{f_{y,T}}{f_y} = \frac{905 - T}{690} \tag{6.6}$$

Incorporating Equation 6.6 into Equation 6.5, Equation 6.7 is obtained.

$$M_{P,T} = S * \frac{905 - T}{690} * f_y \tag{6.7}$$

The beam will no longer support the load applied during the fire when the applied moment M (due to the applied loads) becomes equal to the plastic moment capacities in fire. That is given by the Equation 6.8.

$$M = M_{P,T} \tag{6.8}$$

If the Equation 6.7 re-arranged due to the Equation 6.8, the equation needed to find the plastic moment capacity under fire is obtained. This equation is given by Equation 6.9 down below;

$$\frac{M}{S * f_y} = \frac{905 - T}{690} \tag{6.9}$$

where, $S*f_y$ is the normal temperature plastic moment capacity.

Due to these equations given in the previous page, the critical temperatures and the plastic moment capacity of the beams under elevated temperatures can be found.

6.2.2. Analysis of the Columns Subjected to Four Sided Exposure to Fire

The ratio of strength of columns under elevated temperature conditions to the strength under normal temperature conditions with temperature varies. With the give equations below, it is possible to predict the critical temperature of a column. Also, these equations will generally be conservative. By the help of these equations, it is again possible to obtain the plastic capacity moment of the columns in the frame as well.

To find the critical temperature for the columns in the condition of fire, Equation 6.10 is given below;

$$T_C = 905 - 690 * R \tag{6.10}$$

where, R is the load ratio. Also, the load ratio, R, can be shown as an equation like Equation 6.11.

$$R = \frac{905 - T_C}{690} \tag{6.11}$$

The equation of the plastic moment capacity of the columns in fire condition is as same as the equation of the plastic moment capacity of the beams in fire condition. Therefore, for the columns in the portal frame, the equation becomes the way shown in Equation 6.12.

$$M_{P,T} = S * \frac{905 - T}{690} * f_y \tag{6.12}$$

By the help of these formulas, it is possible to obtain the critical temperatures and the plastic moment capacity for the columns at any given elevated temperature.

6.3. Fire Analysis by Upper-Bound Approach

According to plastic theorems derived for fire situations, the collapse mechanism of a structure occurs when three conditions of equilibrium, mechanism and yield are satisfied. Upper Bound Approach states that a load computed on the basis of an assumed mechanism will always be greater than or at best equal to the true maximum load. This approach is concerned entirely with the determination of the loads at collapse during fire. The deflection of the structure before collapse is totally ignored. The Upper Bound Approach is easy to use for portal frames.

For analysis at elevated temperatures, only the plastic bending moment needs to be adjusted. No thermal loading is to be considered since the plastic collapse load will not be affected by any self-equilibrating loads, such as thermal loads.

The objective of the mechanism method is to select from all possible failure modes of the system, the one that corresponds to the lowest possible plastic limit load. As it is mentioned before, in the previous analysis it is seen that the beam mechanism has given the highest M_p values. According to this result, the beam mechanism will be taken in the fire analysis.

The safety of the example portal frame is to be checked against collapse load factors defined in the approaches. The determination of the collapse mechanism plays a vital role in determination of the collapse temperature. Any non-uniformity of the temperature distribution of the portal steel frame is simulated by two scenarios only in Upper Bound Approach. This is utilized by performing a number of plastic analyses and adopting a common temperature factor, α.

6.3.1. The First Scenario for the Fire Analysis

The first scenario assumes a uniform temperature distribution within the frame. Therefore, all members in the portal frame are assumed to face the same temperature change. The respective temperature distribution within the frame according to the first scenario is given in Figure 6.3 in the next page.

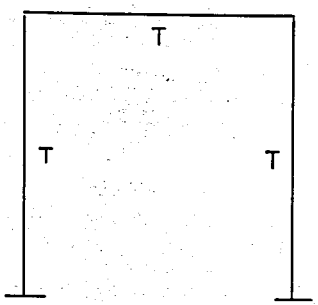

Figure 6.3. Respective temperature distribution within the frame according to scenario 1

Critical mechanism is the beam mechanism in the example portal frame. For the determination of the collapse temperatures for the members, the plastic moment capacities and the yield strengths of the members have to be found at elevated temperatures. These are all calculated by the help of the formulas given before. Also, the load combination for the fire analysis is taken from the Eurocode 3 (EC3, 1995) as G + 0.9 Q for the calculations which gives 8 kN/m. Then, by the help of the virtual work equation, critical plastic load factors, λ_c, are found. Equation 6.13 shows the virtual work equation used in calculations.

$$W_E(ext.work) = W_I(\text{int}.work) \tag{6.13}$$

The results of these calculations are given in the Table 6.1 in the next page. This table shows the yield strengths of the elements at given temperatures, the plastic moment capacities of beams and columns at given elevated temperatures and the collapse load factors at given temperatures. As it is seen from this table, the critical load factor, λ_c, values are decreasing with respect to the increase of the temperature. When the critical load factor, λ_c, reaches the value of 1.0, it means that temperature affecting on the members is the critical temperature for the system. When λ_c (T) = 1, the frame turns into a state of instability even under its working loads and partial or overall collapse may occur. Therefore, according to the first scenario, the frame collapses by the beam mechanism and the critical temperature of the elements determined in this mechanism is 500°C as it is seen from Table 6.1.

As a result of the first scenario, if the uniform temperature distribution exists in the example portal steel frame, the critical temperature for the system would be 500°C. If the

temperature of the frame is greater than 500°C during the fire condition, the system would start to collapse.

Table 6.1. Determination of the collapse temperatures due to the first scenario

SCENARIO 1				
T (°C)	f_{yt} (Kn/m²)	$Mpt_{(col)}$ (Knm)	$Mpt_{(beam)}$ (Knm)	λ_c
50	340760.9	169.49	133.95	2.11
100	320833.3	159.58	126.12	1.98
150	300905.8	149.67	118.29	1.86
200	280978.3	139.76	110.45	1.74
250	261050.7	129.85	102.62	1.61
300	241123.2	119.93	94.79	1.49
350	221195.7	110.02	86.95	1.37
400	201268.1	100.11	79.12	1.24
450	181340.6	90.20	71.28	1.12
500	161413	80.29	63.45	1.00
550	141485.5	70.37	55.62	0.87

6.3.2. The Second Scenario for the Fire Analysis

In the second scenario, this time, it is assumed that all members do not face the same temperature. At the beginning, it is assumed that the initial temperature of the beam of the frame is 100°C whereas the initial temperature of the columns of the frame is 150°C. The temperature which the columns face is shown as T_1 and the temperature which the beam faces is shown as T_2. The relation between these temperatures is shown in Equation 6.14. Also, the respective temperature distribution within the frame according to the second scenario is given in Figure 6.4 below.

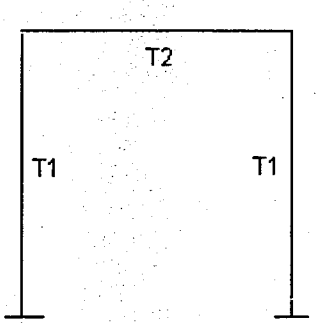

Figure 6.4. Respective temperature distribution within the frame according to scenario 2

$$T_1 = 1.5 * T_2 \qquad (6.14)$$

The difference between the first scenario and the second scenario is the difference between the distributions of the temperatures. In the first one while the distribution is uniform, it is non-uniform in the second scenario. In the determination of the collapse temperature due to the second scenario here, the yield strengths of the elements at given temperatures, the plastic moment capacities of beams and columns at given elevated temperatures and the collapse plastic load factors at given temperatures are calculated once again. Temperatures and corresponding plastic moment capacities of the beams and columns are used again. Again, by the help of the virtual work equation, critical plastic load factors, λ_c, are found.

The results of these calculations according to the second scenario are given in the Table 6.2. As it is seen from the table, the critical load factor, λ_c, reaches the value of 1.05 when the common temperature factor, α, is 3.75. The critical temperature for the beam is 375°C whereas the critical temperature for the columns is 562.5°C.

In this situation, when $\lambda_c (T) \leq 1.05$, the frame turns into a state of instability even under its working loads and partial or overall collapse may occur. Therefore, according to the second scenario, the frame collapses by the beam mechanism again and the critical temperature of the elements determined in this mechanism is 375°C for the beam and 562.5°C for the columns of the portal frame as it is seen from Table 6.2.

As a result of the second scenario, if the non-uniform temperature distribution exists in the example portal steel frame, the critical temperature for the beam and columns would be 375°C and 562.5°C, respectively. If the temperatures of the elements are greater than these values during the fire condition, the system would start to collapse.

So, here again, considering the reduction in the yield strength and the plastic moment capacity the critical temperatures for the beams is 375°C and it is 562.5°C for the columns. As it is mentioned before, if the system exceeds these temperatures, the frame turns into a collapse mechanism.

Table 6.2. Determination of the collapse temperatures due to the second scenario

SCENARIO 2							
α	T_{beam} (°C)	T_{col} (°C)	fyt_{beam} (Kn/m²)	fyt_{col} (Kn/m²)	$Mpt_{(beam)}$ (Knm)	$Mpt_{(col)}$ (Knm)	λ_c
1	100	150	320833.33	300905.80	126.12	149.67	1.92
1.25	125	187.5	310869.57	285960.14	122.20	142.24	1.84
1.5	150	225	300905.80	271014.49	118.29	134.80	1.76
1.75	175	262.5	290942.03	256068.84	114.37	127.37	1.68
2	200	300	280978.26	241123.19	110.45	119.93	1.60
2.25	225	337.5	271014.49	226177.54	106.54	112.50	1.52
2.5	250	375	261050.72	211231.88	102.62	105.07	1.44
2.75	275	412.5	251086.96	196286.23	98.70	97.63	1.36
3	300	450	241123.19	181340.58	94.79	90.20	1.28
3.25	325	487.5	231159.42	166394.93	90.87	82.76	1.21
3.5	350	525	221195.65	151449.28	86.95	75.33	1.13
3.75	375	562.5	211231.88	136503.62	83.04	67.90	1.05
4	400	600	201268.12	121557.97	79.12	60.46	0.97
4.25	425	637.5	191304.35	106612.32	75.20	53.03	0.89

6.4. Second-Order Analysis under Fire by Matrix Theory

6.4.1. Determination of the Values for the Second-Order Analysis under Fire

In frame structures, axial forces act through transverse deflection caused by the bending effect to produce additional deflection and moments in the member which is called as P-Δ effects. In general, there are several simplified methods available for completing second order analysis. Many of the procedures include only P-Δ effects, which is acceptable since the member instability, P-δ effect, is not significant in most structures.

One of the solution procedures which includes frame P-Δ effects is the solution by the 'Stiffness Matrix Method'. By the help of this method it is also possible to find the second order effects of the system under elevated temperatures. The influence of the temperature change in the structure can be taken into consideration whereas the second order effects are considered as well.

First of all, the system's stiffness matrix has to be written from the element matrices according to the 'Code Number Technique'. The system whose stiffness matrix will be

written is shown in Figure 6.5. The numbers shown beside the frame are the number of degree of freedom which will be used in the calculations. The numbers on each element of the frame are the numbers given to the elements.

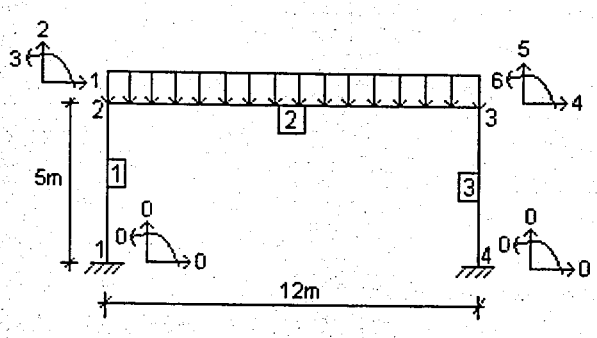

Figure 6.5. The frame system used in 'Stiffness Matrix Theory' solution

The general equation used for the solution of the stiffness matrix of the system is given in Equation 6.15 down below;

$$[K]*\{D\}=\{P\}_{direct}-\sum f \tag{6.15}$$

where,

[K] = System stiffness matrix

{D} = System deformation matrix

$\{P\}_{direct}$ = Direct joint loads acting on the frame

$\sum_f$ = Fixed end reaction vector

To be able to find the system stiffness matrix, element matrices are obtained according to their degree of freedoms. After finding the stiffness matrices for each element, these matrices are combined according to the 'Code Number Technique' and they form the system stiffness matrix. The stiffness matrix belong to the system is given with its values in Equation 6.16.

$$[K]_{XYZ} = \begin{bmatrix} 67010 & 0 & 2192.64 & -66133 & 0 & 0 \\ 0 & 234981 & 367.75 & 0 & -61.29 & 367.75 \\ 2192.64 & 367.75 & 10250.8 & 0 & -367.75 & 1471 \\ -66133 & 0 & 0 & 67010 & 0 & -2192.64 \\ 0 & -61.29 & -367.75 & 0 & 234981 & -367.75 \\ 0 & 367.75 & 1471 & -2192.64 & -367.75 & 10250.8 \end{bmatrix} \quad (6.16)$$

In the example portal frame, there is no direct joint load acting on the frame. Therefore, during the calculations, the value of the direct joint load will be taken zero in the general equation.

The fixed end reaction vector consists of the reaction due to temperature change and uniform loading which is 1.4 G + 1.6 Q in the example portal frame system. Therefore, total fixed end reaction vector can be written as an equation shown below by Equation 6.17;

$$\sum f = f_{temp} + f_{uni} \quad (6.17)$$

where;

f_{temp} = Fixed end reaction due to temperature change

f_{uni} = Fixed end reaction due to the uniform loading acting on the system

The calculations are done for the fixed end reactions acting on the system and the load vectors are obtained separately for the temperature change and the uniform loading. The load vector of the uniform load for the system is given in Equation 6.18.

$$\{f\}_{uni,XYZ} = \begin{bmatrix} 0 \\ 89.4 \\ 178.8 \\ 0 \\ 89.4 \\ -178.8 \end{bmatrix} \quad (6.18)$$

The load vector of the system for the temperature change is obtained as well. While considering the temperature change of the system, the load vectors belong to the beams and the columns are found separately. Afterwards, once again these two load vectors are combined according to the 'Code Number Technique'. The general equations for the beams and the columns under temperature change are given below. Equation 6.19 shows the general equation for the columns and Equation 6.20 shows the general equation for the beams affected by elevated temperature;

$$\{f\}_{col.temp} = \begin{bmatrix} 0 \\ A_c * E * \alpha_t * \Delta T \\ 0 \\ 0 \\ -A_c * E * \alpha_t * \Delta T \\ 0 \end{bmatrix} \tag{6.19}$$

$$\{f\}_{beam.temp} = \begin{bmatrix} A_b * E * \alpha_t * \Delta T \\ 0 \\ 0 \\ -A_b * E * \alpha_t * \Delta T \\ 0 \\ 0 \end{bmatrix} \tag{6.20}$$

where,

A_c = Area of the column section

A_b = Area of the beam section

E = Modulus of elasticity

α_t = Expansion coefficient which is taken $13*10^{-6}$ 1/°C

ΔT = Temperature change

According to the equations above, the load vectors of the elements and then the system will be found. To reach the critical temperature during the fire condition, the ΔT values changes for each increment in the temperature. The initial temperature of the system is the ambient temperature which is 20°C. For every elevated temperature value, the

system has solved once more again. Also, it should be remembered that the value of the modulus of elasticity is changing due to the temperature change in every step. To be able to see all these results found for different degrees, a MATLAB program is written.

After all these solutions, the influence of axial load during fire is taken into consideration as well. By the help of the equations of stability functions, the second-order effects are found. Because of the effect of the stability function coefficients, the system stiffness matrix would change. As a result of this, the system is solved again and again.

For every change in the temperature and the axial loads, the system needs to be analyzed again. It is impossible to do this by hand calculations. Therefore, a MATLAB program which includes the increments of the temperature and the axial load values is written. By the help of this program, the system stiffness matrix is found in every step and the deformations under the second-order effects and fire are obtained. This MATLAB program is written for two different scenarios. These scenarios are the scenarios which are used to find the critical temperature of the system by the Upper-Bound Theorem under fire.

6.4.2. First Scenario for the Second-Order Analysis

In the first scenario, two cases are thought to be analyzed. For the first case, the loading on the frame is uniform as it was before in the first analysis done by the Upper-Bound Theorem under fire. Additionally, the axial load acting on the frame is constant and the temperature is increasing in every step. With these assumptions, the system is solved for each condition by the help of a MATLAB program. Then, the second case which has a changing axial load and increasing temperature at the same time is considered. Another MATLAB program is written for the system with these properties. Again, with these assumptions, the system is solved once again. These MATLAB programs are given below.

All the results for the cases of the first scenario are given in Table 6.3 and 6.4. Also, they are shown in the graphics which are named as Figure 6.6, 6.7 and 6.8. Figure 6.6 shows the temperature versus displacement graphic when the axial load is constant whereas Figure 6.7 shows the temperature versus displacement graphic when the axial load

is changing as well. Figure 6.8 shows the axial force versus displacement, P-Δ, under elevated temperatures.

The MATLAB program for the first scenario when the axial load is constant;

```
close all;
E=2E+8 ; %kn/m2
Ab=39.68E-4 ; %Area of beam section
Ac=58.73E-4 ; %Area of column section
Ib=4.41E-5 ; %Moment inertia of beam
Ic=4.57E-5 ; %Moment inertia of column
Lc=5 ; %Column length
Lb=12 , %Beam length
AlfaT=13E-6 ; %Thermal expansion coefficient
mb=1
nb=0
mc=0
nc=1
Pb=39.75
Pc=89.42
KLb=sqrt(Pb/(E*Ib))*Lb
Fib=2-2*cos(KLb)-KLb*sin(KLb)
eib=KLb*(sin(KLb)-KLb*cos(KLb))/(4*Fib)
eijb=KLb*(KLb-sin(KLb))/(2*Fib)
KLc=sqrt(Pc/(E*Ic))*Lc
Fic=2-2*cos(KLc)-KLc*sin(KLc)
eic=KLc*(sin(KLc)-KLc*cos(KLc))/(4*Fic)
eijc=KLc*(KLc-sin(KLc))/(2*Fic)
% Calculation of stiffness coefficients
Aib=4*E*Ib/Lb*eib
Ajb=Aib*eib
Bb=Aib/2*eijb
Cib=(Aib+Bb)/Lb
Cjb=Cib
Db=(Cib+Cjb)/Lb
Sb=Ab*E/Lb
Aic=4*E*Ic/Lc*eic
Ajc=Aic*eic
Bc=Aic/2*eijc
Cic=(Aic+Bc)/Lc
Cjc=Cic
Dc=(Cic+Cjc)/Lc
Sc=Ac*E/Lc
Kxyz=[((Dc*nc^2+Sc*mc^2)+(Db*nb^2+Sb*mb^2))  ((-Dc*mc*nc+Sc*mc*nc)+(-
Db*mb*nb+Sb*nb*nb))  (Cjc*nc-Cib*nb)  (-Db*nb^2-Sb*mb^2)  (Db*nb*mb-Sb*mb*nb)
(-Cjb*nb) ;
```

```
((-Dc*mc*nc+Sc*mc*nc)+(-Db*mb*nb+Sb*mb*nb))
((Dc*mc^2+Sc*nc^2)+(Db*mc^2+Sb*nb^2)) (-Cjc*mc+Cib*mb) (Db*nb*mb-
Sb*nb*mb) (-Db*mb^2-Sb*nb^2) (Cjb*mb) ;
(Cjc*nc-Cib*nb) (-Cjc*mc+Cib*mb) (Ajc+Aib) (Cib*nb) (-Cib*mb) (Bb) ;
(-Db*nb^2-Sb*mb^2) (Db*nb*mb-Sb*mb*nb) (Cib*nb)
((Db*nb^2+Sb*mb^2)+(Dc*nc^2+Sc*mc^2)) ((-Db*nb*mb+Sb*mb*nb)+(-
Dc*nc*mc+Sc*mc*nc)) (Cjb*nb-Cic*nc) ;
(Db*mb*nb-Sb*mb*nb) (-Db*mb^2-Sb*nb^2) (-Cib*mb) ((-
Db*mb*nb+Sb*mb*nb)+(-Dc*mc*nc+Sc*mc*nc))
((Db*mb^2+Sb*nb^2)+(Dc*mc^2+Sc*nc^2)) (-Cjb*mb+Cic*mc) ;
(-Cjb*nb) (Cjb*mb) Bb (Cjb*nb-Cic*nc) (-Cjb*mb+Cic*mc) (Ajb+Aic) ]
% Load Vector
Funi=[0 ; 89.4 ; 178.8 ; 0 ; 89.4 ; -178.8]
Trans=[0 -1 0 0 0 0 ; 1 0 0 0 0 0 ; 0 0 1 0 0 0 ; 0 0 0 0 -1 0 ; 0 0 0 1 0 0 ; 0 0 0 0 0 1]
T=20
  Et=E*(1+(T /(2000*log(T/1100))))
  DeltaT=T-20
  Fc=[0 ; Ac*Et*AlfaT*DeltaT ; 0 ; 0 ; -Ac*Et*AlfaT*DeltaT ; 0 ]
  Ftempb=[Ab*Et*AlfaT*DeltaT ; 0 ; 0 ; -Ab*Et*AlfaT*DeltaT ; 0 ;0 ]
  Ftempc=Trans*Fc
  Ftemp=Ftempb+Ftempc
  Fsum=Funi+Ftemp
  invKxyz=inv(Kxyz)
D=invKxyz*(-Fsum)
s=D(1,1)
end
```

Table 6.3. Temperature-displacement table when the axial load is constant due to the first scenario

T (°C)	Δ (m)
20	0.1412
50	0.1423
100	0.1441
150	0.1458
200	0.1475
250	0.149
300	0.1504
350	0.1516
400	0.1525
450	0.1532
500	0.1534
550	0.1531
600	0.1521
650	0.1501
700	0.1469
750	0.1417

As it is seen from Table 6.3, when the axial load is constant and the temperature increases in the first case of the first scenario, the deformation values increase until the temperature of the system is 500°C. After 500°C, the deformation values of the system starts to decrease. Therefore, it means 500°C is the critical temperature for the steel portal frame when the second order effects are taken into consideration in the first case of the first scenario.

The MATLAB program for the first scenario when the axial load is changing;

```
clear all;
close all;
E=2E+8 ; %kn/m2
Ab=39.68E-4 ; %Area of beam section
Ac=58.73E-4 ; %Area of column section
Ib=4.41E-5 ; %Moment inertia of beam
Ic=4.57E-5 ; %Moment inertia of column
Lc=5 ; %Column length
Lb=12 , %Beam length
AlfaT=13E-6 ; %Thermal expansion coefficient
mb=1
nb=0
mc=0
nc=1
T=150
Et=E*(1+(T /(2000*log(T/1100))))
DeltaT=T-20
Pb=44.24
Pc=89.42+2.42
KLb=sqrt(Pb/(E*Ib))*Lb
Fib=2-2*cos(KLb)-KLb*sin(KLb)
eib=KLb*(sin(KLb)-KLb*cos(KLb))/(4*Fib)
eijb=KLb*(KLb-sin(KLb))/(2*Fib)
KLc=sqrt(Pc/(E*Ic))*Lc
Fic=2-2*cos(KLc)-KLc*sin(KLc)
eic=KLc*(sin(KLc)-KLc*cos(KLc))/(4*Fic)
eijc=KLc*(KLc-sin(KLc))/(2*Fic)
% Calculation of stiffness coefficients
Aib=4*E*Ib/Lb*eib
Ajb=Aib*eib
Bb=Aib/2*eijb
Cib=(Aib+Bb)/Lb
Cjb=Cib
Db=(Cib+Cjb)/Lb
Sb=Ab*E/Lb
Aic=4*E*Ic/Lc*eic
```

```
Ajc=Aic*eic
Bc=Aic/2*eijc
Cic=(Aic+Bc)/Lc
Cjc=Cic
Dc=(Cic+Cjc)/Lc
Sc=Ac*E/Lc
Kxyz=[((Dc*nc^2+Sc*mc^2)+(Db*nb^2+Sb*mb^2)) ((-Dc*mc*nc+Sc*mc*nc)+(-
Db*mb*nb+Sb*nb*nb)) (Cjc*nc-Cib*nb) (-Db*nb^2-Sb*mb^2) (Db*nb*mb-Sb*mb*nb)
(-Cjb*nb) ;
((-Dc*mc*nc+Sc*mc*nc)+(-Db*mb*nb+Sb*mb*nb))
((Dc*mc^2+Sc*nc^2)+(Db*mc^2+Sb*nb^2)) (-Cjc*mc+Cib*mb) (Db*nb*mb-
Sb*nb*mb) (-Db*mb^2-Sb*nb^2) (Cjb*mb) ;
(Cjc*nc-Cib*nb) (-Cjc*mc+Cib*mb) (Ajc+Aib) (Cib*nb) (-Cib*mb) (Bb) ;
(-Db*nb^2-Sb*mb^2) (Db*nb*mb-Sb*mb*nb) (Cib*nb)
((Db*nb^2+Sb*mb^2)+(Dc*nc^2+Sc*mc^2)) ((-Db*nb*mb+Sb*mb*nb)+(-
Dc*nc*mc+Sc*mc*nc)) (Cjb*nb-Cic*nc) ;
(Db*mb*nb-Sb*mb*nb) (-Db*mb^2-Sb*nb^2) (-Cib*mb) ((-Db*mb*nb+Sb*mb*nb)+(-
Dc*mc*nc+Sc*mc*nc)) ((Db*mb^2+Sb*nb^2)+(Dc*mc^2+Sc*nc^2)) (-Cjb*mb+Cic*mc)
;
(-Cjb*nb) (Cjb*mb) Bb (Cjb*nb-Cic*nc) (-Cjb*mb+Cic*mc) (Ajb+Aic) ]
% Load Vector
Funi=[0 ; 89.4 ; 178.8 ; 0 ; 89.4 ; -178.8]
Trans=[0 -1 0 0 0 0 ; 1 0 0 0 0 0 ; 0 0 1 0 0 0 ; 0 0 0 0 -1 0 ; 0 0 0 1 0 0 ; 0 0 0 0 0 1]
    Fc=[0 ; Ac*Et*AlfaT*DeltaT ; 0 ; 0 ; -Ac*Et*AlfaT*DeltaT ; 0 ]
    Ftempb=[Ab*Et*AlfaT*DeltaT ; 0 ; 0 ; -Ab*Et*AlfaT*DeltaT ; 0 ;0 ]
    Ftempc=Trans*Fc
    Ftemp=Ftempb+Ftempc
    Fsum=Funi+Ftemp
    invKxyz=inv(Kxyz)
D=invKxyz*(-Fsum)
s=D(1,1)
end
```

As it is seen from Table 6.4 in the next page, when the axial load is changing whereas the temperature increases in the second case of the first scenario, the deformation values increase until the temperature of the system is 500°C. As it was in the first case of the first scenario, after 500°C, the deformation values of the system starts to decrease again. Therefore, it means 500°C is the critical temperature again for the steel portal frame when the second order effects are taken into consideration in the second case of the first scenario. All the figures for all cases of the first scenario analysis results are given in the next pages.

Table 6.4. Temperature-displacement table when the axial load is changing due to the first scenario

T (°C)	P_{col} (Kn)	Δ (m)
20	89.42	0.1412
50	139.42	0.1424
100	189.42	0.1444
150	239.42	0.1463
200	289.42	0.1481
250	339.42	0.1498
300	389.42	0.1513
350	439.42	0.1527
400	489.42	0.1538
450	539.42	0.1545
500	589.42	0.1549
550	639.42	0.1548
600	689.42	0.1539
650	739.42	0.1522
700	789.42	0.1489
750	839.42	0.1441
800	889.42	0.1362

When these values which are obtained from the calculations are plotted into the graphics, it is possible to achieve the temperature versus displacement graphic when the axial load is constant due to the first scenario, the temperature versus displacement graphic when the axial load is changing due to the first scenario and the axial force versus displacement graphic due to the first scenario under elevated temperatures.

Again, from all these graphics, it is seen that all of a sudden, the curves start to decrease when the temperature for the two cases is 500°C. Therefore, the critical temperature for the two cases of the first scenario is clearly seen as 500°C from these graphics. That means when the system reaches the temperature of 500°C, the steel portal frame would turn into a state of instability even under its working loads and because of that, the partial or overall collapse may occur in this situation.

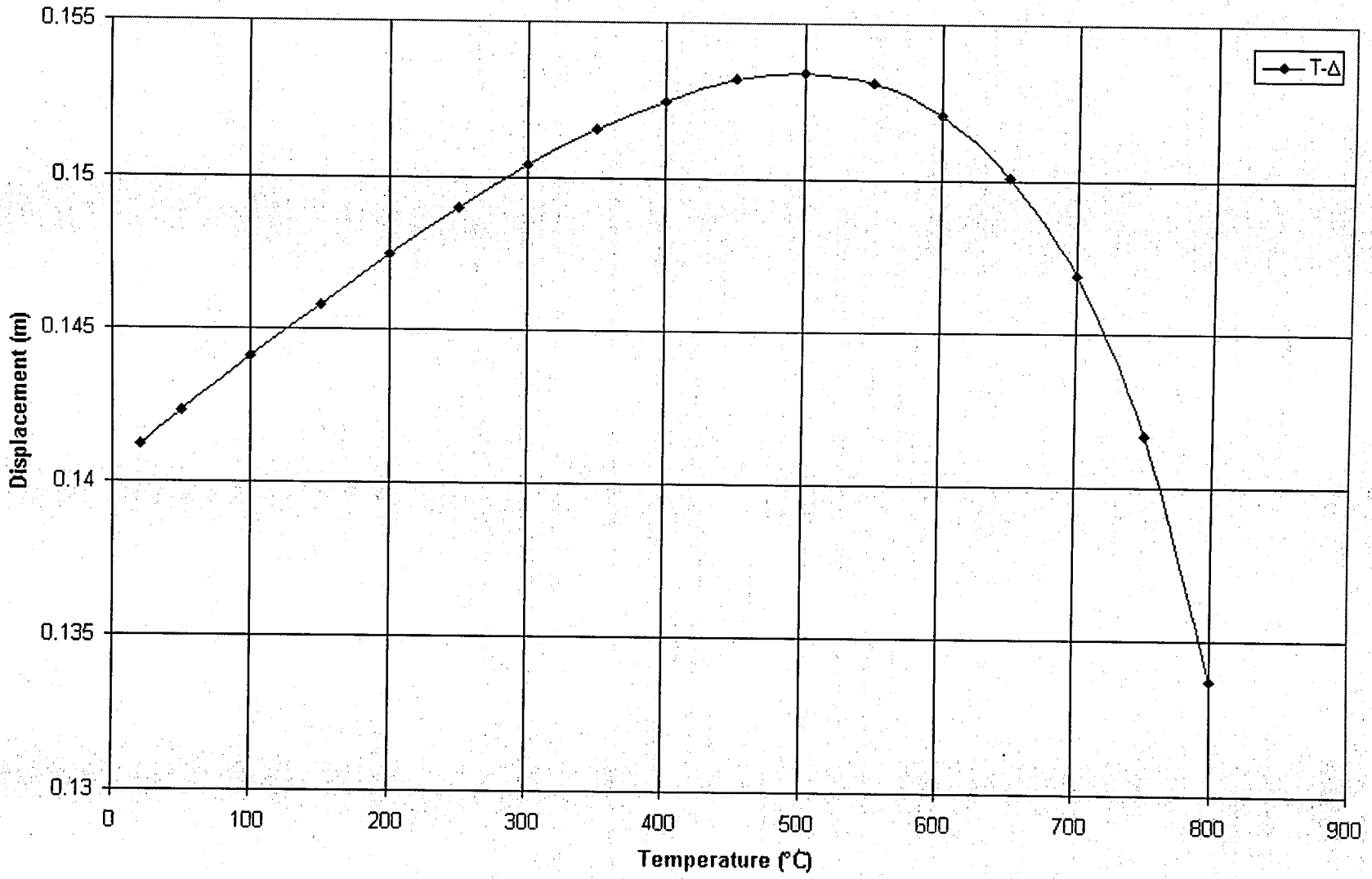

Figure 6.6. Temperature versus displacement graphic when the axial load is constant due to scenario 1

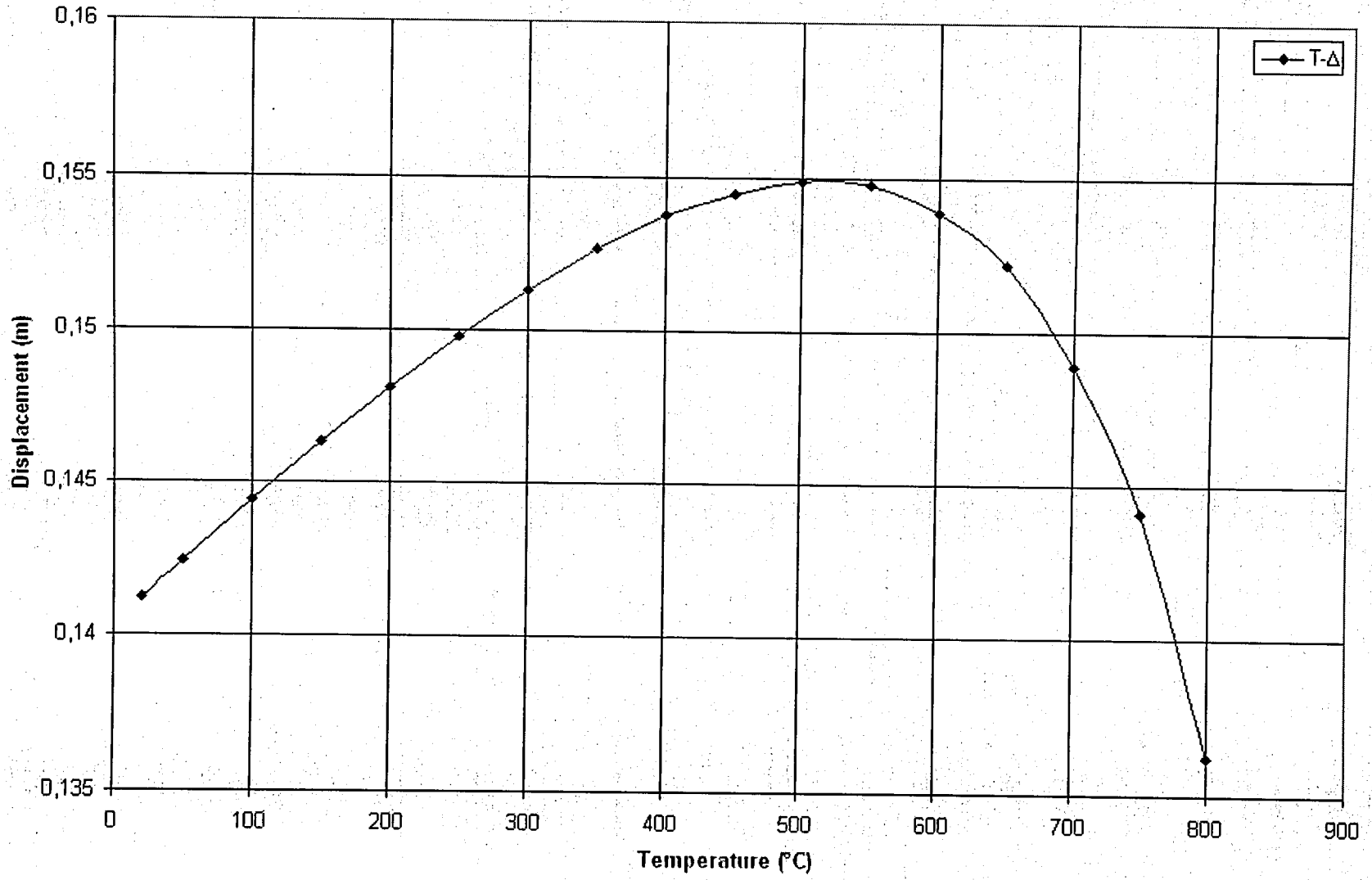

Figure 6.7. Temperature versus displacement graphic when the axial load is changing due to scenario 1

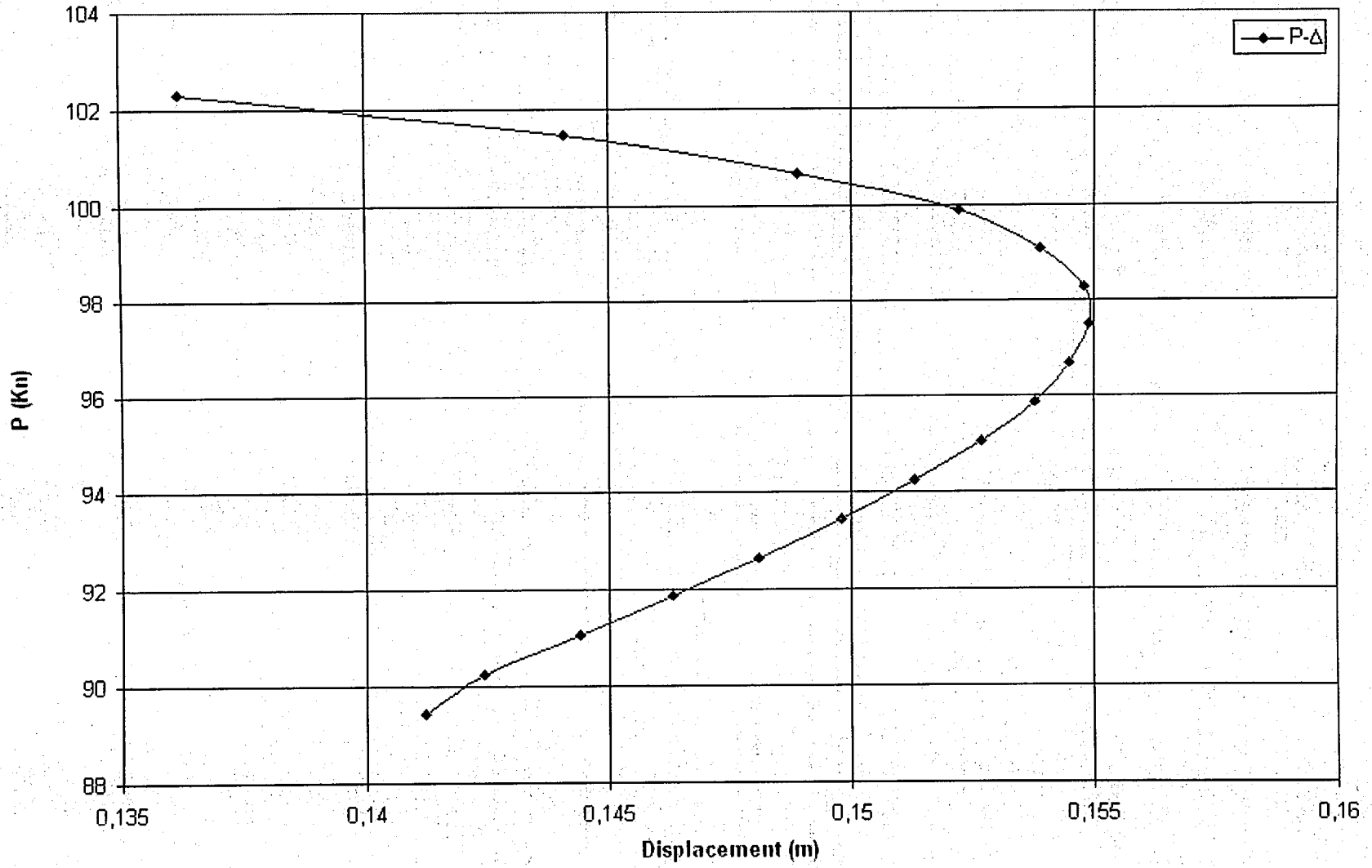

Figure 6.8. Axial force versus displacement due to scenario 1 under elevated temperatures

6.4.3. Second Scenario for the Second Order Analysis

In the second scenario, two cases are thought to be analyzed again. For the first case of the second scenario, the loading on the frame is non-uniform as it was before in the second analysis done by the Upper-Bound Theorem under fire. The temperature distribution on the elements is not uniform like the first scenario. The temperature acting on the columns is 1.5 times more than the temperature acting on the beam. Additionally, in the first case solved for the second scenario, the axial load acting on the frame is constant and the temperature is increasing in every step. For this situation, a MATLAB program is written. With these assumptions, the system is solved for each condition. After that, the second case is determined. According to the second case, the axial load is increased and has taken as a changing axial load. Then, another MATLAB program is written for the system which has a changing axial load and temperature at the same time for the second case. Again, with these assumptions, the system is solved once again. These MATLAB programs are given below.

All the results for the second scenario are given in Table 6.5 and 6.6. Also, they are shown in the graphics which are named as Figure 6.9, 6.10 and 6.11. Figure 6.9 shows the temperature versus displacement graphic when the axial load is constant whereas Figure 6.10 shows the temperature versus displacement graphic when the axial load is changing as well. Figure 6.11 shows the axial force versus displacement, P-Δ, under elevated temperatures due to the second scenario.

The MATLAB program for the second scenario when the axial load is constant;

```
clear all;
close all;
E=2E+8 ; %kn/m2
Ab=39.68E-4 ; %Area of beam section
Ac=58.73E-4 ; %Area of column section
Ib=4.41E-5 ; %Moment inertia of beam
Ic=4.57E-5 ; %Moment inertia of column
Lc=5 ; %Column length
Lb=12 , %Beam length
AlfaT=13E-6 ; %Thermal expansion coefficient
mb=1
nb=0
```

```
mc=0
nc=1
Pb=39.75
Pc=89.42
KLb=sqrt(Pb/(E*Ib))*Lb
Fib=2-2*cos(KLb)-KLb*sin(KLb)
eib=KLb*(sin(KLb)-KLb*cos(KLb))/(4*Fib)
eijb=KLb*(KLb-sin(KLb))/(2*Fib)
KLc=sqrt(Pc/(E*Ic))*Lc
Fic=2-2*cos(KLc)-KLc*sin(KLc)
eic=KLc*(sin(KLc)-KLc*cos(KLc))/(4*Fic)
eijc=KLc*(KLc-sin(KLc))/(2*Fic)
% Calculation of stiffness coefficients
Aib=4*E*Ib/Lb*eib
Ajb=Aib*eib
Bb=Aib/2*eijb
Cib=(Aib+Bb)/Lb
Cjb=Cib
Db=(Cib+Cjb)/Lb
Sb=Ab*E/Lb
Aic=4*E*Ic/Lc*eic
Ajc=Aic*eic
Bc=Aic/2*eijc
Cic=(Aic+Bc)/Lc
Cjc=Cic
Dc=(Cic+Cjc)/Lc
Sc=Ac*E/Lc
Kxyz=[((Dc*nc^2+Sc*mc^2)+(Db*nb^2+Sb*mb^2)) ((-Dc*mc*nc+Sc*mc*nc)+(-
Db*mb*nb+Sb*nb*nb)) (Cjc*nc-Cib*nb) (-Db*nb^2-Sb*mb^2) (Db*nb*mb-Sb*mb*nb)
(-Cjb*nb) ;
((-Dc*mc*nc+Sc*mc*nc)+(-Db*mb*nb+Sb*mb*nb))
((Dc*mc^2+Sc*nc^2)+(Db*mc^2+Sb*nb^2)) (-Cjc*mc+Cib*mb) (Db*nb*mb-
Sb*nb*mb) (-Db*mb^2-Sb*nb^2) (Cjb*mb) ;
(Cjc*nc-Cib*nb) (-Cjc*mc+Cib*mb) (Ajc+Aib) (Cib*nb) (-Cib*mb) (Bb) ;
(-Db*nb^2-Sb*mb^2) (Db*nb*mb-Sb*mb*nb) (Cib*nb)
((Db*nb^2+Sb*mb^2)+(Dc*nc^2+Sc*mc^2)) ((-Db*nb*mb+Sb*mb*nb)+(-
Dc*nc*mc+Sc*mc*nc)) (Cjb*nb-Cic*nc) ;
(Db*mb*nb-Sb*mb*nb) (-Db*mb^2-Sb*nb^2) (-Cib*mb) ((-Db*mb*nb+Sb*mb*nb)+(-
Dc*mc*nc+Sc*mc*nc)) ((Db*mb^2+Sb*nb^2)+(Dc*mc^2+Sc*nc^2)) (-
Cjb*mb+Cic*mc);
(-Cjb*nb) (Cjb*mb) Bb (Cjb*nb-Cic*nc) (-Cjb*mb+Cic*mc) (Ajb+Aic) ]
% Load Vector
Funi=[0 ; 89.4 ; 178.8 ; 0 ; 89.4 ; -178.8]
Trans=[0 -1 0 0 0 0 ; 1 0 0 0 0 0 ; 0 0 1 0 0 0 ; 0 0 0 0 -1 0 ; 0 0 0 1 0 0 ; 0 0 0 0 0 1]
T=20
Etb=E*(1+(T /(2000*log(T /1100))))
Etc=E*(1+(1.5*T /(2000*log((1.5*T)/1100))))
DeltaTc=1.5*T-20
DeltaTb=T-20
```

```
Fc=[0 ; Ac*Etc*AlfaT*DeltaTc ; 0 ; 0 ; -Ac*Etc*AlfaT*DeltaTc ; 0 ]
Ftempb=[Ab*Etb*AlfaT*DeltaTb ; 0 ; 0 ; -Ab*Etb*AlfaT*DeltaTb ; 0 ;0 ]
Ftempc=Trans*Fc
Ftemp=Ftempb+Ftempc
Fsum=Funi+Ftemp
invKxyz=inv(Kxyz)
D=invKxyz*(-Fsum)
s=D(1,1)
end
```

Table 6.5. Temperature-displacement table when the axial load is constant due to the second scenario

T_{beam} (°C)	T_{col} (°C)	Δ (m)
20	30	0.1423
50	75	0.1451
100	150	0.1495
150	225	0.1533
200	300	0.1565
250	375	0.1585
300	450	0.1589
350	525	0.1569
400	600	0.1512
450	675	0.1394
500	750	0.1174
550	825	0.076

As it is seen from Table 6.5 above, when the axial load is constant whereas the temperature increases, the deformation values increase as well until the temperature of the beam is 300°C and the temperature of the column is 450°C. After these temperature degrees which belong to the elements of the steel portal frame, the deformation values starts to decrease. Therefore, it means 300°C is the critical temperature for the beam and 450°C is the critical temperature for the columns in the system when the second order effects are taken into consideration in the first case of the second scenario.

The MATLAB program for the second scenario when the axial load is changing;

```
E=2E+8 ; %kn/m2
Ab=39.68E-4 ; %Area of beam section
Ac=58.73E-4 ; %Area of column section
Ib=4.41E-5 ; %Moment inertia of beam
```

```
Ic=4.57E-5 ; %Moment inertia of column
Lc=5 ; %Column length
Lb=12 , %Beam length
AlfaT=13E-6 ; %Thermal expansion coefficient
mb=1
nb=0
mc=0
nc=1
T=600
Etb=E*(1+(T /(2000*log(T/1100))))
Etc=E*(1+(1.5*T /(2000*log((1.5*T)/1100))))
DeltaTb=T-20
DeltaTc=1.5*T-20
Pb=39.75+17.96
Pc=89.42+14.49
KLb=sqrt(Pb/(E*Ib))*Lb
Fib=2-2*cos(KLb)-KLb*sin(KLb)
eib=KLb*(sin(KLb)-KLb*cos(KLb))/(4*Fib)
eijb=KLb*(KLb-sin(KLb))/(2*Fib)
KLc=sqrt(Pc/(E*Ic))*Lc
Fic=2-2*cos(KLc)-KLc*sin(KLc)
eic=KLc*(sin(KLc)-KLc*cos(KLc))/(4*Fic)
eijc=KLc*(KLc-sin(KLc))/(2*Fic)
% Calculation of stiffness coefficients
Aib=4*E*Ib/Lb*eib
Ajb=Aib*eib
Bb=Aib/2*eijb
Cib=(Aib+Bb)/Lb
Cjb=Cib
Db=(Cib+Cjb)/Lb
Sb=Ab*E/Lb
Aic=4*E*Ic/Lc*eic
Ajc=Aic*eic
Bc=Aic/2*eijc
Cic=(Aic+Bc)/Lc
Cjc=Cic
Dc=(Cic+Cjc)/Lc
Sc=Ac*E/Lc
Kxyz=[((Dc*nc^2+Sc*mc^2)+(Db*nb^2+Sb*mb^2)) ((-Dc*mc*nc+Sc*mc*nc)+(-
Db*mb*nb+Sb*nb*nb)) (Cjc*nc-Cib*nb) (-Db*nb^2-Sb*mb^2) (Db*nb*mb-Sb*mb*nb)
(-Cjb*nb) ;
((-Dc*mc*nc+Sc*mc*nc)+(-Db*mb*nb+Sb*mb*nb))
((Dc*mc^2+Sc*nc^2)+(Db*mc^2+Sb*nb^2)) (-Cjc*mc+Cib*mb) (Db*nb*mb-
Sb*nb*mb) (-Db*mb^2-Sb*nb^2) (Cjb*mb) ;
(Cjc*nc-Cib*nb) (-Cjc*mc+Cib*mb) (Ajc+Aib) (Cib*nb) (-Cib*mb) (Bb) ;
(-Db*nb^2-Sb*mb^2) (Db*nb*mb-Sb*mb*nb) (Cib*nb)
((Db*nb^2+Sb*mb^2)+(Dc*nc^2+Sc*mc^2)) ((-Db*nb*mb+Sb*mb*nb)+(-
Dc*nc*mc+Sc*mc*nc)) (Cjb*nb-Cic*nc) ;
```

```
(Db*mb*nb-Sb*mb*nb) (-Db*mb^2-Sb*nb^2) (-Cib*mb) ((-Db*mb*nb+Sb*mb*nb)+(-
Dc*mc*nc+Sc*mc*nc)) ((Db*mb^2+Sb*nb^2)+(Dc*mc^2+Sc*nc^2)) (-Cjb*mb+Cic*mc)
(-Cjb*nb) (Cjb*mb) Bb (Cjb*nb-Cic*nc) (-Cjb*mb+Cic*mc) (Ajb+Aic) ]
% Load Vector
Funi=[0 ; 89.4 ; 178.8 ; 0 ; 89.4 ; -178.8]
Trans=[0 -1 0 0 0 0 ; 1 0 0 0 0 0 ; 0 0 1 0 0 0 ; 0 0 0 0 -1 0 ; 0 0 0 1 0 0 ; 0 0 0 0 0 1]
    Fc=[0 ; Ac*Etc*AlfaT*DeltaTc ; 0 ; 0 ; -Ac*Etc*AlfaT*DeltaTc ; 0 ]
    Ftempb=[Ab*Etb*AlfaT*DeltaTb ; 0 ; 0 ; -Ab*Etb*AlfaT*DeltaTb ; 0 ;0 ]
    Ftempc=Trans*Fc
    Ftemp=Ftempb+Ftempc
    Fsum=Funi+Ftemp
    invKxyz=inv(Kxyz)
D=invKxyz*(-Fsum)
s=D(1,1)
end
```

Table 6.6. Temperature-displacement table when the axial load is changing due to the second scenario

T_{beam} (°C)	T_{col} (°C)	P_c (Kn)	Δ (m)
20	30	89.42	0.1412
50	75	89.9	0.1424
100	150	90.63	0.1452
150	225	91.84	0.1498
200	300	93.04	0.1538
250	375	94.25	0.1571
300	450	95.46	0.1593
350	525	96.67	0.1599
400	600	97.87	0.158
450	675	99.08	0.1525
500	750	100.29	0.1409
550	825	101.5	0.1191

For the second case in the second scenario, it is observed from the Table 6.6 above that when the axial load is increasing whereas the temperature increases at the same time, the deformation values increase until the temperature of the beam is 350°C and the temperature of the column is 525°C. After these temperature degrees which belong to the elements of the steel portal frame, it is seen that the deformation values starts to decrease. Therefore, it means 350°C is the critical temperature for the beam and 525°C is the critical temperature for the columns in the system when the second order effects are taken into consideration in the second case of the second scenario.

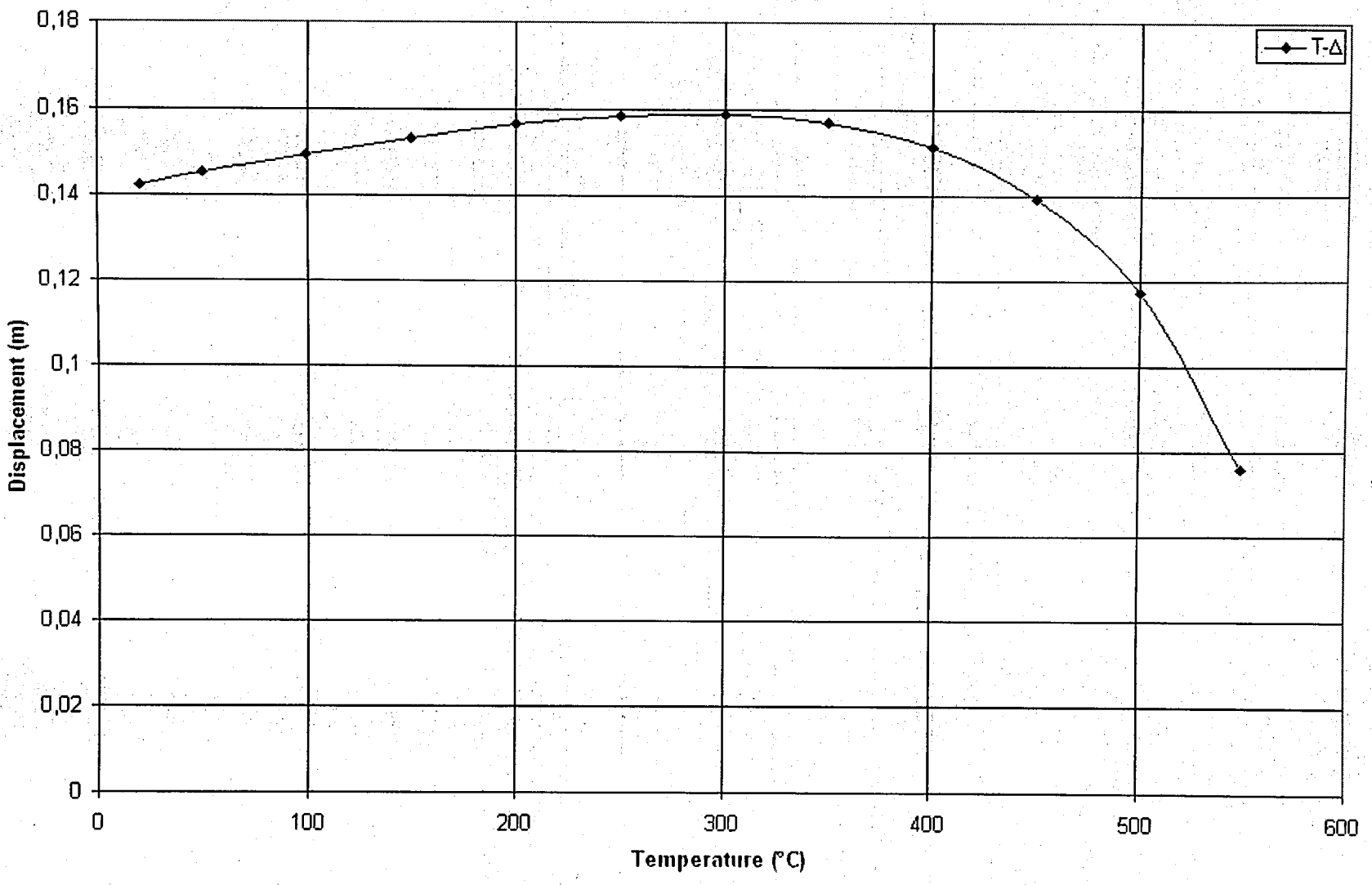

Figure 6.9. Temperature versus displacement graphic when the axial load is constant due to scenario 2

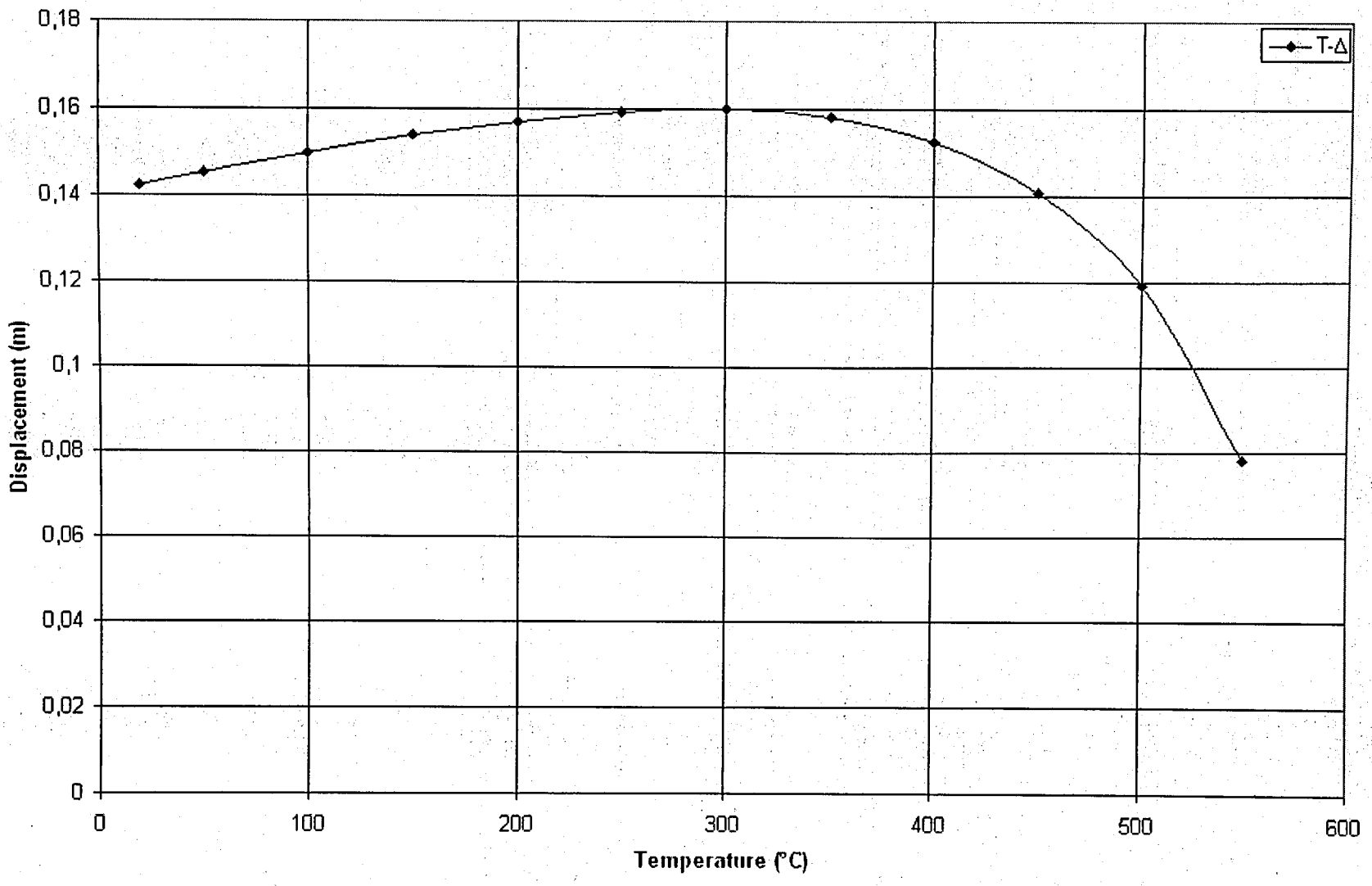

Figure 6.10. Temperature versus displacement graphic when the axial load is changing due to scenario 2

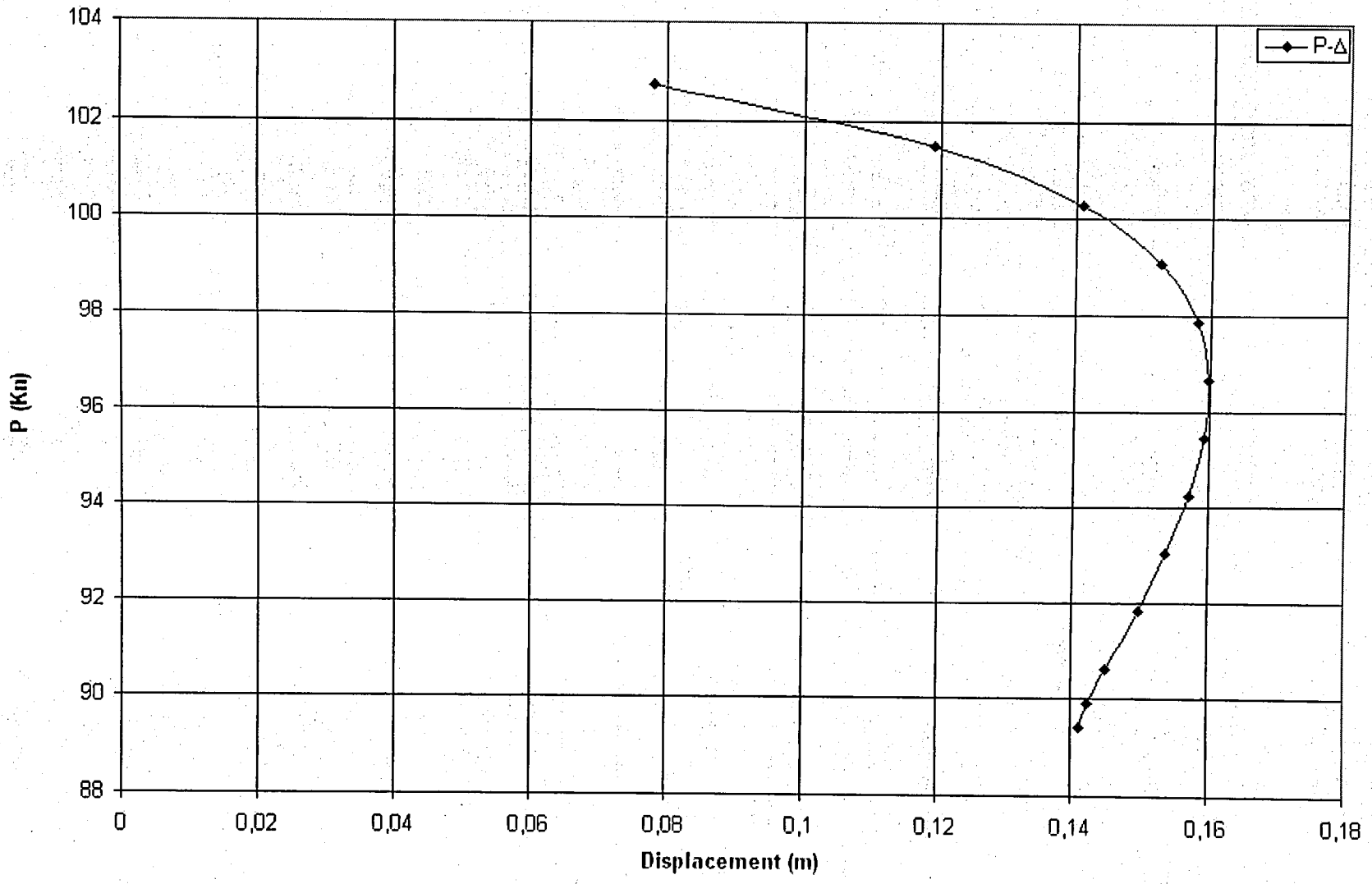

Figure 6.11. Axial force versus displacement due to scenario 2 under elevated temperatures

7. CONCLUSIONS

Severe fires in large buildings are rare and unpredictable events, but when they occur, they can cause great damage and loss of life. Structural design for fire is a small but important part of the overall process of providing fire safety in buildings. Safer buildings can help to reduce the risk of loss of life and property in the event of an unwanted fire.

In the present study, because of the importance of the fire event on structures, a portal steel frame is analyzed under elevated temperatures. In the first analysis method, the Upper-Bound Theorem which is one of the three classical plastic theorems has been successfully extended to fire analysis. The Upper Bound Theorem states that the collapse temperature is an upper bound when only the mechanism condition is satisfied, regardless of the equilibrium condition. The time concept or the duration of the fire is not taken into account in the study. Only the collapse or the critical temperature according to assumed scenarios is obtained. However, this study reveals the critical temperature, to which the members of the frame should not reach at any fire occasion. Hence, it can be proposed that a sufficient coverage of members or precautions such as sphinxters to avoid the increase in the temperature of the frame members can be utilized as means of fire protection.

According to the first scenario done by the Upper Bound Theorem, it is seen that if a uniform temperature distribution within the members of the frame is assumed, the collapse mechanism of the frame at ambient temperature does not vary as the temperature increases during a fire event. Therefore, the plastic moment capacity value in the equation of the collapse mechanism is important when a different distribution is postulated. Also, the location of the plastic hinges plays a vital role in the mathematical definition of the load factors and the critical temperature. Therefore, a careful inspection of change in the plastic moment capacities of the members with respect to temperature is required as well.

The collapse temperature of the system in the first scenario would be 500°C due to the analysis done. That means, if the temperature of the frame is greater than 500°C during the fire condition, the system would start to collapse. Therefore, the members of the example frame should not reach this critical temperature at a fire scenario like this.

As it is known, in the second scenario, the temperature distribution which the columns in the system face is 1.5 times more than the temperature distribution which the beams face. When the temperature distribution of the frame members is taken into account by these assumptions done for the second scenario, the critical temperature for the beam and columns would be 375°C and 562.5°C, respectively, due to the Upper Bound Theorem. If the temperatures of the elements are greater than these values during the fire condition, the system would start to collapse.

When the results are compared, it is seen that the distribution of the temperature increment in the system is important. The critical temperature for the elements and the system changes according to the distribution of the temperature in the system which can not be known during a fire. So, as a result of the fire analysis done by the Upper Bound Theorem, it is seen that if a distribution of initial member temperatures and the function which defines the increase under fire conditions are given or assumed, then the collapse mechanism and the critical temperature of collapse can be calculated.

The second order effects are particularly important in framed structures. If the system is multistory building, the axial forces would be larger. Then, the secondary effect becomes significant and should be included in the analysis of the structure for sure. But in single storey portal frames, the secondary effects are negligible. Therefore, it is unnecessary to take the second order effects into consideration. But in this study, although the second order effects are negligible in single portal frames, considering the extra effect of elevated temperatures, the system is analyzed under second order effects as well.

For the second order effect analysis of the system under elevated temperatures, two scenarios are assumed again. In the first scenario, the system is faced to a uniform distribution of elevated temperature whereas it is faced to a non-uniform distribution in the second one. Each scenario has two cases. In the first cases, the axial load acting on the system is constant whereas in the second case, the axial load acting on the system is increasing as well. The critical temperatures of collapse for each scenario and each case are shown in Table 7.1 in the next page.

Table 7.1. The critical temperatures of the elements for each scenario and each case

	SCENARIO 1		SCENARIO 2	
	$T_{c,col}$ (°C)	$T_{c,beam}$ (°C)	$T_{c,col}$ (°C)	$T_{c,beam}$ (°C)
$P_{constant}$	500	500	450	300
$P_{changing}$	500	500	525	350

As it is seen from Table 7.1 in the first scenario, even there is the axial load difference in each case, the critical temperature stays the same. On the other hand, for the second scenario, it is seen that the critical temperature changes due to the axial load increment. The deflections caused by the effect of the axial loads in critical temperatures are given in Table 7.2 for each case of the scenarios.

Table 7.2. Deflections and critical temperatures of the elements for each case and each scenario

	SCENARIO 1			SCENARIO 2		
	Δ (m)	$T_{c,col}$ (°C)	$T_{c,beam}$ (°C)	Δ (m)	$T_{c,col}$ (°C)	$T_{c,beam}$ (°C)
$P_{constant}$	0.1534	500	500	0.1589	450	300
$P_{changing}$	0.1549	500	500	0.1599	525	350

It is concluded that the axial deformations in the members have little difference between each other in every case of the scenarios. As it is mentioned before, in single storey portal frames, the secondary effects are too small to be considered. But when there is an extra effect of fire condition on the system, axial load effect changes the critical temperatures. Therefore, second order analysis has to be done as well to see how much the critical temperature of collapse changes.

When the critical temperature results obtained by the Upper Bound Theorem and the Second Order Analysis compared with each other, it is seen that the results are different from each other and that both analysis should be done to find the most critical temperature for the system. These two analysis methods results are given in Table 7.3 down below. As it is seen from Table 7.3, in the first scenario, the critical temperature is 500°C found for

both of the analysis methods. Both analyses give the same critical temperature of collapse for the system due to the assumptions. On the other hand, when the elevated temperature distribution is not constant in the second scenario, the results differ from each other for each analysis methods. It is seen that the results found by the help of the Upper Bound Theorem gives the most critical temperature value for the system during fire.

Table 7.3. The comparison of the critical temperatures obtained by each theorem

	SCENARIO 1		SCENARIO 2	
	$T_{c,col}$ (°C)	$T_{c,beam}$ (°C)	$T_{c,col}$ (°C)	$T_{c,beam}$ (°C)
Upper Bound Theorem Results	500	500	562.5	375
Second Order Analysis Results $P_{constant}$	500	500	450	300
Second Order Analysis Results $P_{changing}$	500	500	525	350

As a result of this study, although the critical temperature is obtained by the Upper Bound Theorem for the example portal frame in this study, the second order analysis has to be still done to be sure of the critical temperature that the system would reach. It is understood that under fire condition, the Upper Bound Theorem can serve as a quick tool to determine the fire resistance of steel frames.

Also, the analytical results indicate that the stability and the second order response of framed structures are not only affected by the magnitude of the axial load, but also by the increment of the temperatures as well.

REFERENCES

Anderberg, Y., 2003, "Design Methods and Structural Performance", Course in Udine, Italy.

Anderberg, Y., 2003, "Thermal Properties and Analysis of Steel", Course in Udine, Italy.

Anderberg, Y., 2003, "Fire Scenarios and Buildings", Course in Udine, Italy.

Bennetts, I. D., D. J. Proe and I. R. Thomas, 1987, *Guidelines for Assessment of Fire Resistance of Structural Steel Members*, Australian Institute of Steel Construction, AISC.

Bennetts, I. D. and K. W. Poh, 1995, "Analysis of Structural Members Under Elevated Temperature Conditions", *Journal of Structural Engineering*, Vol. 121, pp. 664-675.

British Standard Institution (BSI), 1985, *Structural Use of Steelwork in Building*, Part 1, BS5950.

British Standard Institution (BSI), 1990, *Code of Practice for Fire Resistant Design*, Part 8, BS5950.

Buchanan, A. H., 2000, *Structural Design for Fire Safety*, New York.

Chen, W. F. and E. M. Lui, 1986, *Structural Stability: Theory and Implementation*, New York.

Chen, W. F. and I. Sohal, 1995, *Plastic Design and Second Order Analysis of Steel Frames*, New York.

Eurocode 3 (EC3), 2001, *Design of Steel Structures: Part 1.2. General Rules-Structural Fire Design (EC3-1.2)*, Commission of European Communities, Brussels, Belgium.

Neal, B. G., 1963, *The Plastic Methods of Structural Analysis*, New York.

Rubert, A. and P. Schaumann, 1986, "Structural Steel and Plane Frame Assemblies Under Fire Action", *Fire Safety Journal*, Vol.10, pp. 173-184.

Skowronski, W., 1997, "Plastic Load Capacity and Stability of Frames in Fire", *Engineering Structures*, Vol. 19, pp. 764-771.

Tang, C. Y. and K. H. Tan, 2001, "Basis and Application of Simple Interaction Formula for Steel Frames Under Fire Conditions", *Journal of Structural Engineering*, Vol. 127, pp. 1214-1220.

Toh, W. S., T. C. Fung and K. H. Tan, 2001, "Fire Resistance of Steel Frames Using Classical and Numerical Methods", *Journal of Structural Engineering*, Vol. 127, pp. 829-838.

Toh, W. S., T. C. Fung and K. H. Tan, 2001, "Strength and Stability of Steel Frames in Fire: Rankine Approach", *Journal of Structural Engineering*, Vol. 127, pp. 461-469.

TS 498, 1987, *Design Loads for Buildings*, Turkish Standards Institute, Ankara.

TS 500, 2000, *Requirements for Design and Construction of Reinforced Concrete Structures*, Turkish Standards Institute, Ankara.

Turkish Earthquake Code (TEC 98), 1998, *Specification for Structures to be Built in Disaster Areas*, Ministry of Public Works and Settlement, Government of Republic of Turkey.

Usmani, A. S. and J. M. Rotter, 2001, "Fundamental Principles of Structural Behaviour Under Thermal Effects", *Fire Safety Journal*, Vol.36.

Vimonsatit, V., K. H. Tan and S. K. Ting, 2003, "Plastic Limit Temperatures of Flexibly Connected Steel Frames: A Linear Programming Problem", *Journal of Structural Engineering*, Vol. 129, pp. 79-86.

Wang, Y. C. and D. B. Moore, 1995, "Steel Frames in Fire: Analysis", *Engineering Structures*, Vol. 17, pp. 462-472.

Wong, M. B., 2001, "Elastic and Plastic Methods for Numerical Modelling of Steel Structures Subject to Fire", *Journal of Constructional Steel Research*, Vol. 57, pp. 1-14.

Wong, M. B., 2001, "Plastic Frame Analysis Under Fire Conditions", *Journal of Structural Engineering*, Vol. 127, pp. 290-295.

STEEL FRAMES UNDER FIRE

by

Işıl Sanrı

B.S. in C.E., Çukurova University, 2001

Submitted to the Institute for Graduate Studies in
Science and Engineering in partial fulfillment of
the requirements for the degree of
Master of Science

Graduate Program in Civil Engineering
Boğaziçi University

2004

STEEL FRAMES UNDER FIRE

APPROVED BY:

Prof. Gülay Altay
(Thesis Supervisor) .....

Prof. Turan Özturan .....

Assoc. Prof. Cavidan Yorgun .....

DATE OF APPROVAL: 12/05/2004